EAFIT UNIVERSITY

Engineering School

Design Engineering Research Group (GRID)

Process of Component Integration for Concentrating Photovoltaic Systems

Graduation manuscript presented as partial requirement to obtain the

Master in Engineering

(Draft Document: Version 16/06/2017)

AUTHOR:

David Esteban González Correa, Eng.

ADVISOR - COAUTHOR:

Gilberto Osorio Gómez, PhD.

June 2017

Contents

List of Figures

List of Tables

Abstract

This document proposes a new methodical process to design and integrate CPV systems considering real efficiencies of the components and including environmental and process variables.

Concentrating Photo Voltaic (CPV) systems maximize energy harvested from the sun with multi-junction solar cells of less area, reducing related implementation costs and reaching energy production thresholds up to 38,9%. Nowadays, CPV systems are generally implemented in solar energy farms in a permanent location, however, these systems could be used in other dynamic contexts, such as vehicles or portable devices. In this way, mechanical and geometrical parameters related to manipulation, transportation and installation should be carefully considered at the design stage. Besides, each condition of use presents different variables affecting these parameters. In all, there is not an established architecture for these systems, opening up the possibility of radically changing their use, geometry and components.

Therefore, a methodical process for designing of CPV systems is proposed in order to predict their behavior in terms of implementation and energy production. This might allow the development of robust concepts that can be adapted to different context of use as required, providing an itinerant character and thus extending the field of implementation of these systems beyond a static use. The relevant variables for the use of CPV systems are determined through experimentation considering the implementation of Fresnel lenses as light concentrators. This allows generating a structured design guide composed of different methods of measurement, selection and development. The methodical process is based on a perspective of functional modules considering needs, technical aspects and particular usage conditions of each design and it would provide appropriate guidelines in each circumstance.

Keywords: Concentrating Photo Voltaic (CPV), Fresnel lens, Alignment process, Design and assembly, Context of use, Tolerances ratio (TR), Performance Index

Acknowledgements

I would first like to thank my thesis advisor PhD Gilberto Osorio Gómez from the Department of Product Design Engineering at EAFIT University because, despite the setbacks, inconvenients, and sleepless nights experienced during the development process of this project, I could always count on him, with his great ability as a brilliant professional and his advice as a human being. I thank him for his good guidance during this great journey.

I would like to thank PhD Ricardo Mejía, director of GRID (Research Group of Product Design Engineering) at EAFIT University, whose demand has pushed me to go further and further to overcome and break my own paradigms.

I thank my colleagues, who accompanied me in the process of developing the solar vehicle in parallel to this project and of those who i learned so much about all aspects of life, especially Mauricio Fernández, David Acevedo and Esteban Betancur.

Thanks to EAFIT University for hosting me in its campus and providing me with the necessary tools to achieve all my objectives and to develop myself fully as a professional, and special thanks to Empresas Públicas de Medellín for making possible the scholarship that I used to advance my masters studies.

I would also like to thank my colleagues from GRID and all those who participated during this process through their opinions and feedback during the group's presentations. Thanks to their suggestions, I was able to enrich this work until a pleasant culmination of it.

I must deeply thank my friends Simón Galeano, Carolina Correa and Sara López since they helped me unselfishly during the experimentation and testing phase to be able to finish this work in the expected time for it.

Finally, I must express my great gratitude and love to my parents and my family for providing me with unfailing support and continuous encouragement throughout my years of study and through the research and writing process of this document. This achievement would not have been possible without them.

Thank you.

David Esteban González Correa

Chapter 1

Introduction

1.1 Context

"A Concentrating Photo Voltaic (CPV) system converts light energy into electrical energy in the same way that conventional photovoltaic technology does, but it uses an advanced optical system to focus a large area of sunlight onto each cell for maximum efficiency as it is shown in Figure 1.1 [19]. Different CPV designs exist, sometimes differentiated by the concentration factor, such as low-concentration (LCPV) and high concentration (HCPV)". [4]

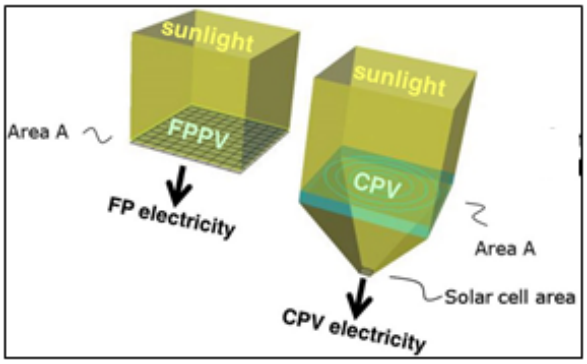

Figure 1.1: CPV systems replace solar cell plates with a panel of optical elements that concentrate sunlight into a set of small solar cells of high-performance [19].

There are many types of CPVs differentiated by their components, architecture or physical configuration and some values of characteristic parameters as it is shown in Figure 1.2.

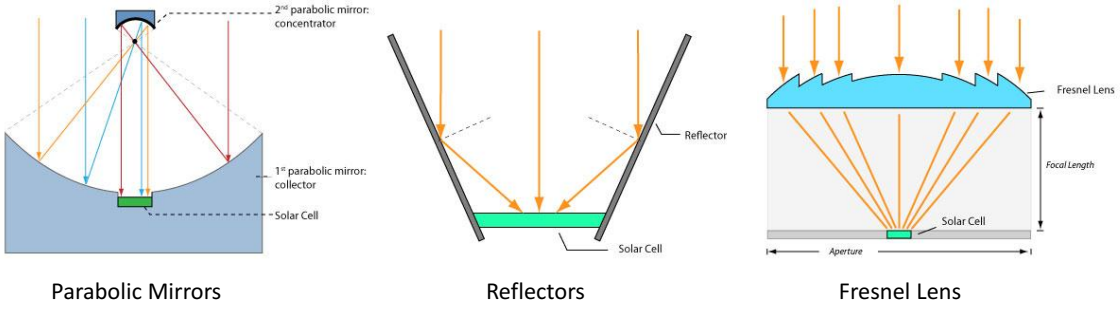

Figure 1.2: Some types of optical elements used for CPV systems [15].

A CPV has three essential components: first, an optical element that can work by refraction or reflection to redirect and concentrate the sunlight, so this element can be a lens or a mirror with different forms and geometries. The second component is the photovoltaic element that transforms the sunlight redirected by the optical element in electrical energy and, for these applications, this is usually a high-performance small solar cell of GaAs or multi-junction. The last component is an interface element, which integrates the other components to define the final geometry of the CPV. This last element varies according to the CPV type or optical element used. The implementation of various CPVs in a same interface element integrates a functional module allowing the achievement of high energy standards specifically developed for punctual requirements. This description of components is shown in Figure 1.3.

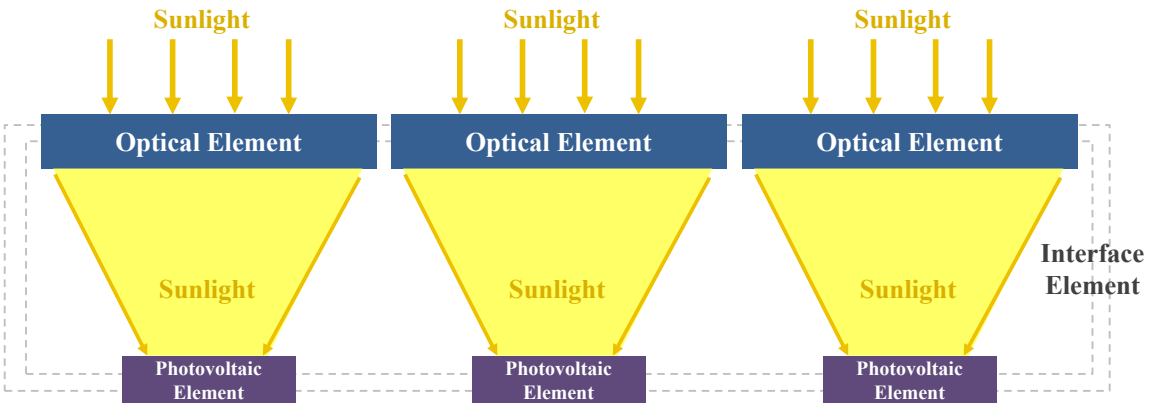

Figure 1.3: Main components of a functional module of CPVs.

By implementing these systems properly, a better balance of cost/benefit ratio is achieved, obtaining increased energy production without incurring in the high cost associated with photovoltaic elements. However, the implementation of the concentration systems brings new challenges related with parameters and exclusive conditions of use, which have been studied and solved progressively seeking to strengthen the use of this technology.

It should be mentioned that the CPV systems generally come with a solar alignment or a solar tracker system [3] because they work exclusively with the component of direct light from the sun, i.e., the rays of light coming out from the sun and enter the optical element perpendicularly. Therefore, this relative position should ensure the operation of the system all the time. This type of solar aligners has been vastly studied and currently various related technological developments are presented, where active components represent an energy expenditure of the system. In this sense, the component of the weight of CPV systems is important because in order to move more weight it is required a greater energy expenditure, also, lighter systems facilitate handling on the part of operators or final users.

The parameters governing the performance of the CPV systems vary to some extent by the elements used and their functional principles. However, for more configurations there are parameters that can be generalized. Anyway, elements that most variation present are the optical ones, and this type of components has behaviors defined by the same physical principles.

One of the most important parameters in all CPV systems is the Concentration Factor (CF), defined in Equation 1.1, that determines the level of energy production of the system and corresponds to the ratio between the area of the optical element and the area of the photovoltaic element [3].

$$CF = \frac{Optical\ element\ area}{Photovoltaic\ element\ area} \tag{1.1}$$

According to Chemisana, there are three main levels of CF: high concentration factor when the factor is greater than 100 ($CF > 100$), medium concentration factor when the factor is between 10 and 100 ($10 < CF < 100$) and low concentration factor when the factor is less than 10 ($CF < 10$) [3].

High CF allows theoretically much greater energy production; however, systems with these configurations have higher requirements. On the one hand, a factor of very high concentration also represents a high temperature, which could result in degradation in the solar cell if the temperature is not properly controlled; on the other hand, these concentration factors determine a parameter known as the acceptance angle. According to Chemisana, high concentration factors always require a solar tracker of two axes with a margin of error in the acceptance angle less to 0.2°, while the middle and lower factors have lower tolerances and can work with trackers of a single axis or even eliminate these systems [3].

Although this parameter is common in any CPV system, the use of certain optical elements or certain usage configurations facilitates or restricts the reach of high concentration factors because for these levels it is required the most possible difference between the optical and photovoltaic areas. So, in optical systems with line focus or line-shaped, the difference of areas is much smaller compared to optical systems with shaped focus point. These configurations are shown in Figure 1.4 with Fresnel lenses of line and point focus on the left and reflectors or parabolic mirrors of line and point focus on the right [3].

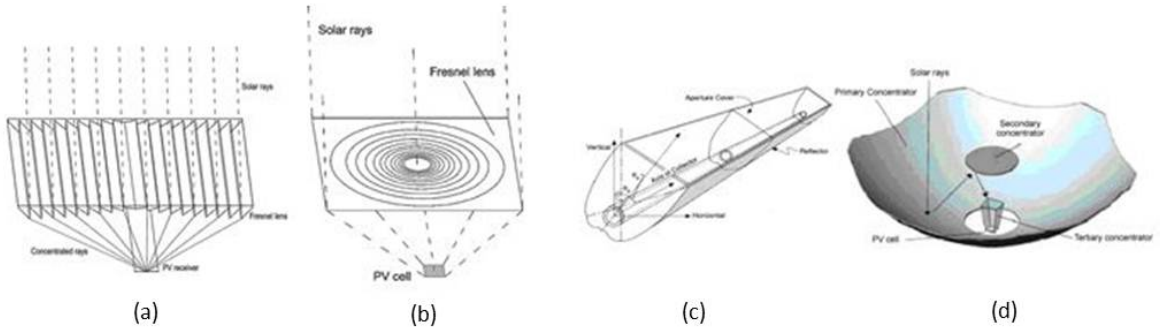

Figure 1.4: (a) CPV with Fresnel lens and line focus, (b) CPV with Fresnel lens and point focus, (c) CPV with parabolic mirror and line focus and (d) CPV with parabolic mirror and point focus [3]

.

Other important parameters, such as the angle of acceptance which represents the tolerance of the perpendicularity of the system to the sun, or the focal length which must be ensured between the optical element and the photovoltaic element to focus the light exactly on the photovoltaic cell, are related directly to the internal alignments of the components that must be guaranteed by the manufacturing method and the tools used to perform the assembly and must be preserved at the time of CPV use. In Figure 1.5 the most relevant general parameters for CPV systems are summarized.

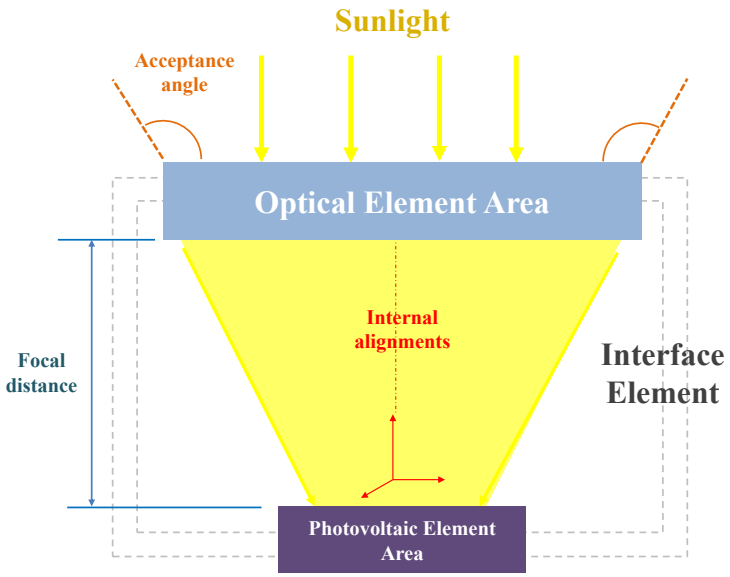

Figure 1.5: Main parameters of a CPV.

1.2 Problem Definition

In order to capture as much energy as possible with a CPV system, there must be a precise alignment between the used optical systems and photovoltaic cells, which is achieved through a strategy of assembly and alignment that allows finding the position of better efficiency of the cell in relation to the focal point of light. Likewise, it is evident the need to develop an interface element that serves to integrate other components, giving structural character and a defined architecture to the CPV and preserving alignment conditions according to the design and conditions of use. The implications of bad processes of design, manufacturing, assembly and alignment are illustrated in Figure 1.6.

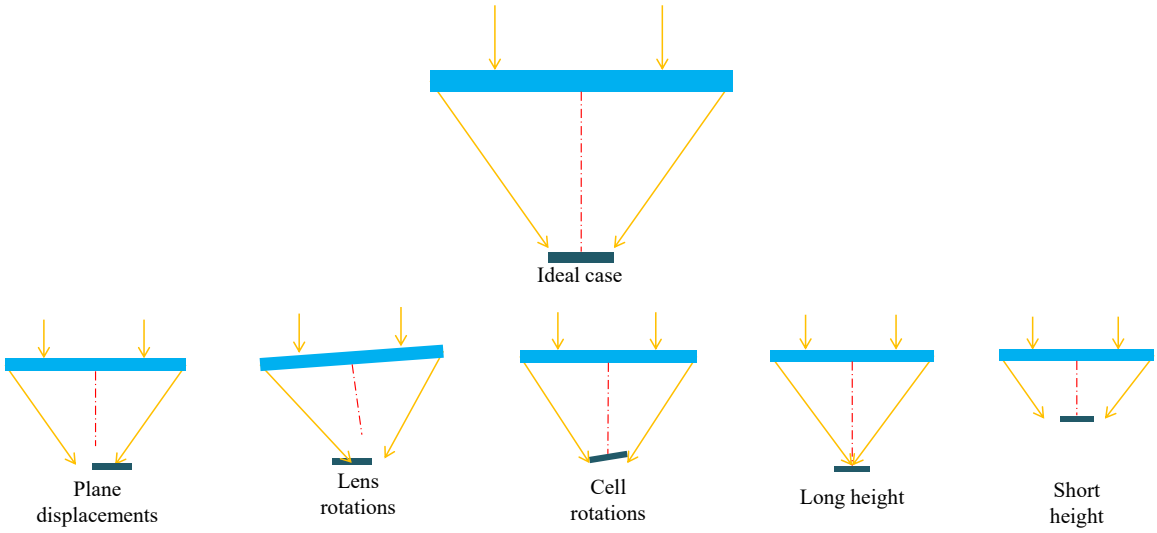

Figure 1.6: Assembly errors that can be present in CPVs.

1.3 Research Question

How to improve the design process of a concentrating photovoltaic system that is stored and transported to work in different places, in order to improve its performance ?

1.4 Objectives

1.4.1 General Objective

Develop a methodical process for the design and integration of components for foldable concentration photovoltaic systems for place changes through the integration of tools and methods for the control of the main variables that affect the behavior of the system in order to determine an adjusted energy production.

1.4.2 Specific Objectives

- Identify internal and external variables that affect the energy production of foldable concentration photovoltaic systems for place changes.
- Define steps for the designing and assembly of CPVs based on existing methods of product design, manufacture and assembly.

- Determine methods and tools of control and characterization of the main variables that affect the CPV systems.
- Develop an experiment design to validate the methods and tools used in the methodical process of integration and design.
- Validate the methodical process through groups of test and interviews.

1.5 Definitions and Scope

- Modularity facilitates folding and change place and is determined by the space requirements.
- Satisfying the most demanding environmental conditions allows functionality in the specified placements in the Product Design Specifications (PDS).

The design and integration method for CPVs is delimited by the PDS delivered at the beginning of the project. This document directs research efforts, defines previously selected components in a process external to this project and sets the basis for the identification of the most relevant variables that impact the system in relation to some characteristics of use, such as roaming.

The development of this project includes the design of an interface component that integrates the different components and provides structurality to the CPV. It also includes the design and development of possible tools necessary for the assembly processes of the components. Solar tracking systems for the implementation of modules are excluded from the design. For the specific purposes of this project it is assumed that sunlight is always perpendicular to a reference plane parallel to CPVs.

As a final scope, it is expected to create a method, or descriptive and detailed step-by-step, for designing CPVs in an easy, agile and reliable manner that can be generalized and applied to several types of similar systems and that provides the necessary tools to determine the most important factors for any CPV design.

Chapter 2

State of the Art

2.1 Introduction

For several decades, CPV systems have been the center of attention of institutions and researchers around the world [30]. However, only in recent years this knowledge has been moved to industry which has begun to market these systems, presenting them as a real highly useful alternative that offers great benefits compared to traditional photovoltaic systems, as they have the potential to reduce costs associated with the production of solar energy, by making it more affordable and competitive in terms of renewable energy. This, added to a model for large-scale energy production, can lead to a significant increase in cost-benefit terms.

Contemporary companies like "SEMPRIUS", "MORGAN SOLAR", "AIRLIGHT", "AZUR SPACE" and "SOITEC" manufacture and market CPV systems and high efficiency photovoltaic cells as it is shown in Figure 2.1 [27]. Most of these companies are focused on solar power plants and large-scale installations, including solar tracking system and assembly and installation services. Most commonly used optical technologies are the Fresnel lenses, plane-convex lenses and parabolic mirrors or faceted parabolic mirrors. [4] [7] [11] [27] [28] [29]

Figure 2.1: CPV module manufactured and power plant installed by SEMPRIUS. [27]

Latest applications for CPV technology are oriented to power mobile systems. Under these circumstances, additional parameters and conditions are considered, as the weight of the components, exposure to adverse environmental conditions, among other external factors. This must be understood to achieve an appropriate and efficient operation.

Institutions and space agencies, like NASA, have been working with developments based on CPV technologies to maximize the energy gain that can be obtained from the sun and used for the operation of satellites and space vehicles as it is shown in Figure 2.2 [3].

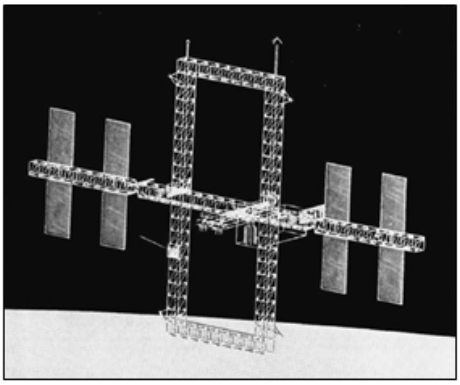

Figure 2.2: Satellite powered by CPVs [3].

Similar uses in mobile systems have been presented in recent years with the creation of solar vehicles of high efficiency with CPVs, for automotive competitions, as it is shown in Figure 2.3 [1], where the results of the most recent research and technological advances associated with this subject are used and applied.

Figure 2.3: Solar vehicle energized by CPVs [1].

2.2 Focus of Lenses

The main manufacturers of CPV systems for high-energy production plants use Fresnel or plane-convex lenses showed in Figure 2.4 [10]. However, these elements have facilitated the development of CPV technology of smaller scale, through smaller functional units that can be integrated, strengthening more their scalability for different approaches.

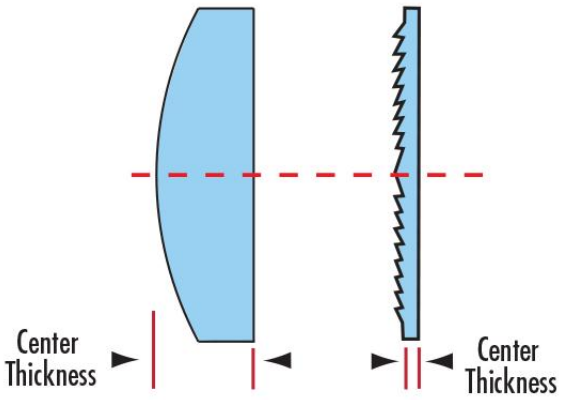

Figure 2.4: Plane-convex lens (left) and Fresnel lens (right). [10]

Plane-convex lenses have good optical efficiency allowing the penetration of most light into the cell except what it is lost by absorbance due to the material properties of the lens. Nevertheless, the biggest disadvantage of the plane-convex lenses is its large volume due to the relationship between the diameter and height of the lens for a given focal point. This situation limits the dimensions of these elements by weight and production cost, limiting the possibility of achieving high concentration factors with largest photovoltaic cells. [30]

Meanwhile, Fresnel lenses allow to reach a wide range of concentration factors varying the diameter of the lens freely without disproportionate increasing in weight and production cost. Although they

have little less efficiency compared with plane-convex lenses, this loss can be included in the functional model of the systems to overcome it.

The application of technologies such as CPV systems have promoted the creation of companies that develop and distribute Fresnel lenses with a variety of options; including lenses designed specifically for solar concentration. Thanks to their thin geometry, companies have been able to make developments in different materials such as PMMA or PC, materials that do not affect significantly the optical properties of lenses compared with glass, but reduce its weight and fragility. This market simplifies the process of design and development of CPV systems eliminating the need to design and produce their own lenses.

2.3 State of the Art

In order to propose a methodical process of design, manufacture and assembly, it was decided to focus the proposal on CPV systems with Fresnel lens due the exposed advantages. To develop the proposal it was necessary to study existing methods and tools for the development of CPVs and how the different variables and parameters are analyzed and integrated in these processes.

In the framework of this research, existing methods of development and assembly of CPV systems, based on refractive optical elements such as Fresnel lenses or plane-convex lenses, have been identified. Such research has been focused on the three basic elements configuring a CPV, Photovoltaic Element, Optical Element and Interface Element. In addition, methods and tools used to align CPV systems and, finally, existing methods to determine the impact of different variables related to the use conditions and manufacture of CPV systems based on design and assembly tolerances, were studied.

2.3.1 Methods of Development and Assembly of CPV Systems Based on Refractive Optical Elements

In terms of technological development, two approaches are clearly characterized in the design and manufacture of CPVs based in refracting optical elements.

The first is the development of a highly industrialized level CPVs with micro-components. These CPVs are currently governing the market and are developed by companies like "SEMPRIUS" or "SOITEC" [27] [28]. These use highly technological and automated processes based on printing methods and Surface Mount Technology (SMT) [9] [26]. These methods are traditionally used for electronic assemblies on a small-scale (micrometers or millimeters) requiring high precision, giving this type of CPVs a robust character that improves efficiency, reliability and performance.

Despite their great benefits, such CPVs are highly expensive and their manufacture requires very specialized and complex machinery, which represents a significant barrier if manufacturers want

to implement these processes for local development of CPVs. Figure 2.5 shows a CPV module of "SEMPRIUS". [27]

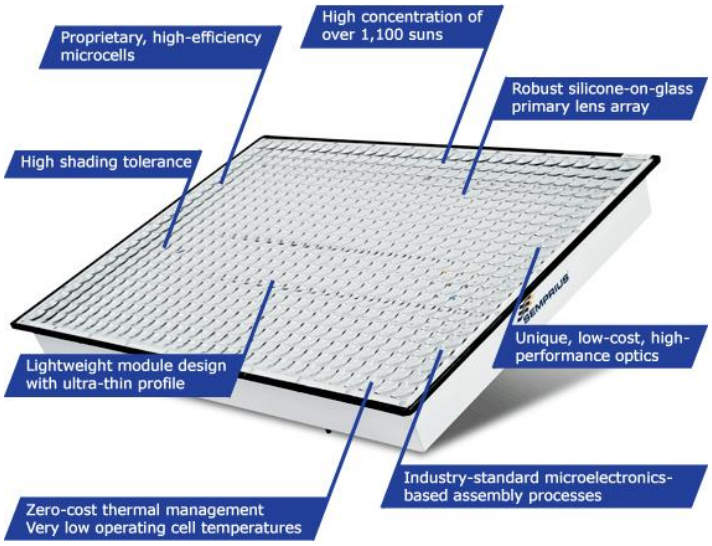

Figure 2.5: CPV module manufactured by SEMPRIUS. [27]

As far as photovoltaic cells are concerned, this type of development has a clearly marked electronic approach, which directs the manufacturing processes mainly towards the manufacture and assembly of the photovoltaic cell, generally of Gallium as the main semiconductor material, and the manufacture and assembly of the lower plate of the module as an integrated circuit board that allows the electrical connections between cells and the other components to be reached. Developments are also disclosed in plate type thermal dissipation systems, also manufactured on the surfaces of the back plate due to the high concentration factors to which these CPVs are usually subjected [17] [9].

Information about these CPVs does not present details about the primary lens, their manufacture and proper assembly in relation to the photovoltaic cell and just indicates the use of panels of Fresnel lenses or plane-convex lenses aligned with the cells. However, most of these CPVs present in their design the use of secondary lenses, whether in the form of a sphere, a dome or a tetrahedron as it is shown in Figure 2.6. These lenses are assembled in self-supporting printed structures with respect to the photovoltaic cell and adhered on its surface creating an airtight seal. These elements increase the acceptance angle of the CPV in relation to light beams reducing the degree of precision required to assemble and align the primary lens relative to the cell, also distributing homogeneously the light incident on the photovoltaic cell to improve the performance of the system [17] [9] [26].

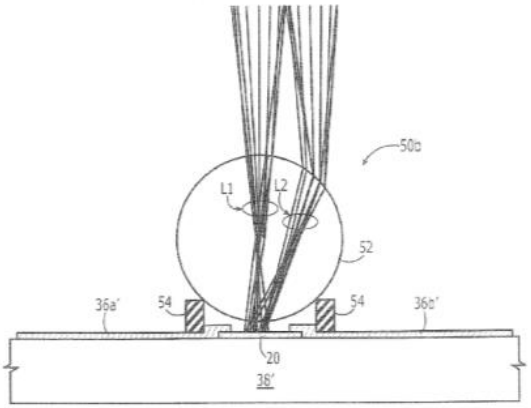

Figure 2.6: Spherical secondary lens (caption 52) for increase the light acceptance angle [17].

For the interface element or chassis, these designs have a geometry of tray-type formed in one piece and in various plastic and metal materials. This kind of chassis has bearing surfaces at the edges to assemble the primary lenses and create together a closed functional module but there are not many details of this. Figure 2.7 shows an example of typical shape chassis. [26]

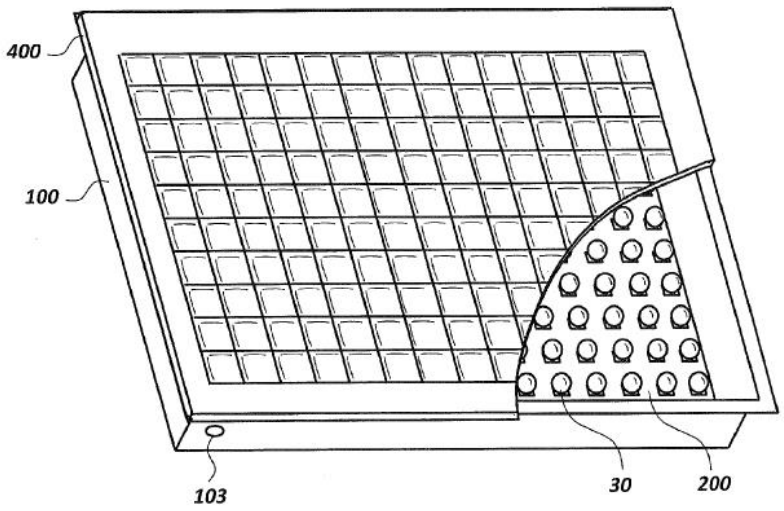

Figure 2.7: CPV module with tray type chasis. [26].

These types of CPVs are the most functional and advanced in terms of the processes and technologies that are used to shape them. The use of micro components and continuous forms in one piece give them greater structural integrity with less weight but access to these technologies is expensive and complicated as they are generally marketed in large quantities and for almost exclusive use of solar farms.

A second approach of development of CPVs is based on less sophisticated and automated processes where larger scale components are used and essentially a process of integration of components may be defined, as it is presented in Figure 2.8. these developments are not industrialized products and are presented from research and prototypes, focused on the different components of the CPVs, lenses, cells and chassis. [18] [8] [12] [22]

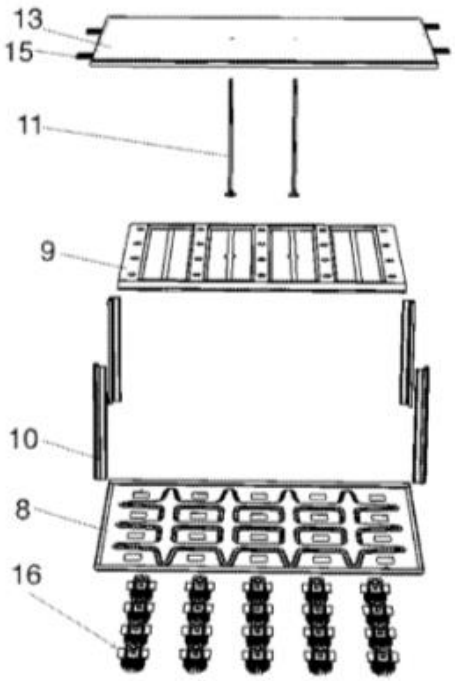

Figure 2.8: Exploded view of a CPV module. (16: solar collector, 8: Base, 10: Columns of the comer, 9: Protection against misalignment situations of the lens, 11: Central stiffening columns, 13: Lens, 15: Fastening pieces of the module to the solar) [12].

Generally, modules of photovoltaic cell ready for connection and installation are used and, in some cases, assembled in thermal dissipation structures and with secondary lenses, as optical elements such as it is shown in Figure 2.9 [12] [18] .

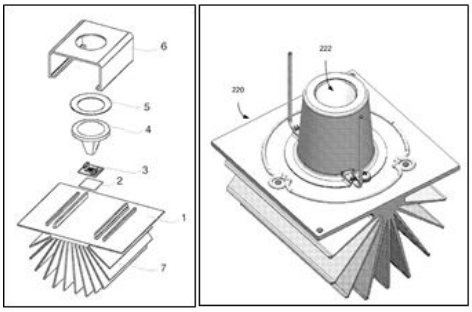

Figure 2.9: Solar collectors made up of a photovoltaic cell, a secondary lens and a heat sink. (7: Fins, 1: Heat sink, 2: Thermal paste, 3: Receiver, 4: Secondary optics, 5: Washer, 6: Fastening piece of the solar collector) [12] [18].

As main optical elements these CPVs mostly use fresnel lenses in the form of panels of several lenses as well as individual lens assemblies as it is shown in Figure 2.10 [18][20][22].

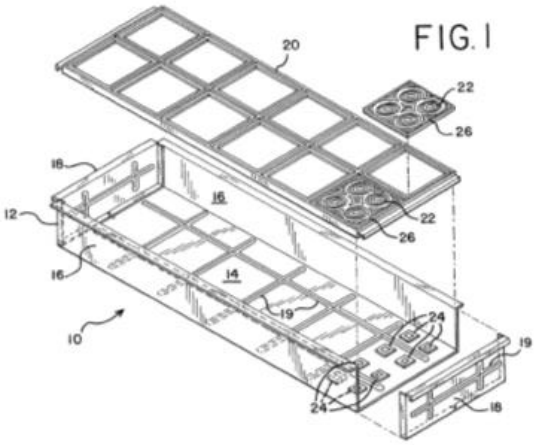

Figure 2.10: Fresnel lens assembly for CPV module. [22]

The interface element or chassis of these designs presents the form of boxes and, most times, the faces are developed separately and assembled with mechanical elements or adhesives. Sometimes these CPVs have frames in rigid materials, such as steel, in order to integrate walls of lighter materials [8] [12] [18] [22].

Assembly and alignment processes of these CPVs are based primarily on the development of components manufactured through CNC technologies that ensure greater precision in the pieces that can be used as aligners. Sometimes the use of jigs, dies or external fixtures, like work tables previously aligned and designed, is specified to provide reference structures for the assembly of CPVs. Kinematic joints, conical aligners or reference holes are used to ensured exact positions of the parts which are assembled with mechanical components such as rivets, screws or adhesives. Lenses are aligned using

lasers properly positioned perpendicularly to show focal points, besides using guides and reference surfaces [18] [20] [22].

The lower plate of the modules usually have the precise holes for the assembly of the photovoltaic cells as it is shown in Figure 2.11 [18], allowing to realize the pattern of cells of homogeneous form to later assemble the primary lenses on these[12].

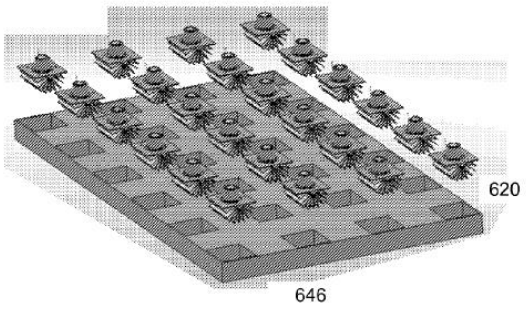

Figure 2.11: Jig hole for alignment of solar collectors. [18]

The process of assembly and alignment of primary lenses can be done in two ways, through the alienating elements previously aligned with respect to the cell and located at the edges of the walls of the modules where the lenses will rest. This method has the disadvantage that it does not include dimensional differences between lenses which can result in an accumulation of error as the lenses are assembled, causing possible differences between the behaviors of the photovoltaic cells within the module. Then, it is important to ensure that the position of each lens is accurate, aligned and the same with respect to each cell [18][12].

The other way to align the primary lenses with the cells is by means of lasers. Using this method it is necessary to ensure that the light beam of the lasers is perpendicular with respect to the lenses. Some developments achieve this by adjusting the laser in a chassis with screws and placing a reflective surface on the lenses, so when the light beam of the laser is perpendicular to the surface, the reflection of this must coincide with the output of the laser. When it is certain that the lasers are perpendicular to the lenses, the center location of the photovoltaic cell can be determined with respect to the light source generated by the lens [18].

The designs of CVPs based on this second approach present more variety of shapes and components and use simpler and easier to process and assemble methods and assembly tools. However, the simplifications of these CPVs present some disadvantages that must be tackled simplifying manufacturing processes. Reliability is compromised in terms of the functionality of the modules and in order to simplify components, such as lenses or chassis, the number of individual parts is usually increased, making the assembly more complicated in terms of tolerances and raises the need to use a greater

number of assembly components by increasing the final weight of the modules and reducing their structural integrity.

It is suggested to determine a mixed process where continuous parts and rigid structural materials are fabricated for the interface element or chassis, but based assembly methods and tools in the second CPVs design approach allow to replicate the processes more easily and these may be subject to improved practices such as the inclusion of electronic tools, sensors to ensure better tolerances between parts or improve the accuracy of the necessary alignments.

2.3.2 Methods and Tools Used for Aligning Optical Elements for CPV Systems

Methods and tools, with more information from the literature, for alignment of concentration systems have been developed especially for systems with faceted mirrors [25]. In terms of alignment with lenses of CPVs there is very little information. However, some of the methods found can be adapted for use in aligning lenses of CPVs.

Starting with the most basic methods like visual alignment or alignment with inclinometers where simple accessible tools are used and sometimes for not depending on the sun, lasers are used to perform visual alignments. These systems are easy to implement and are not expensive, but the alignment processes can take a lot of time and it has a greater possibility of error by the person involved [25].

Position Sensing Detector (PSD) are often used as precision systems in combination with lasers and prisms, and, more recently, cameras and systems of image processing have been used as methods of photogrammetry and fringe reflection, making developments of specialized software to refine alignment processes through computer media [25]. Some methods for alignment are presented in Figure 2.12 [25].

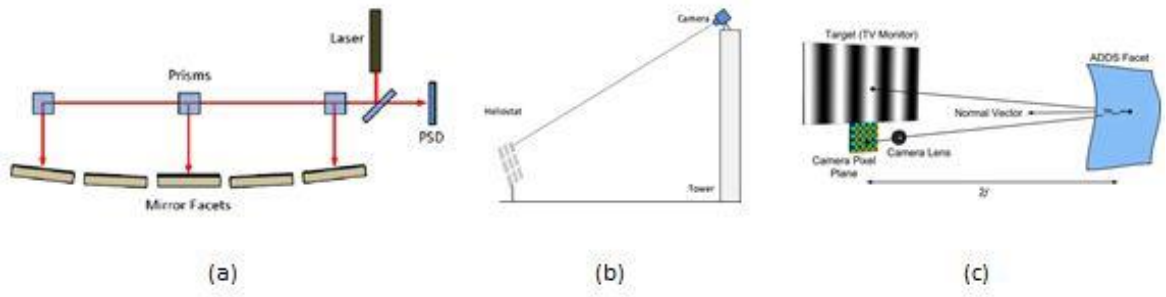

Figure 2.12: Some methods for alignments of mirrors, (a) Scanning prism laser projection method, (b) Camera look-back method and (c) Fringe reflection method [25].

2.3.3 Methods for Measuring Impact of Variables Related to the Use Conditions and Manufacture of CPV Systems

Numerical methods and analysis of computational models can perform simulations of cases and scenarios to determine the impact of different conditions and variables on the behavior of the modeled systems. This is the case of "MORGAN SOLAR INC.", where a sensitivity analysis process, supported by a simulation tool called MSOS, simulates the impact of different parameter values to determine the performance of the systems developed. Such analysis is presented in Figure 2.13. In this way, it is possible to see the most sensitive points in the development, assembly and implementation process of systems and identify the most influential parameters without making constant real tests [6].

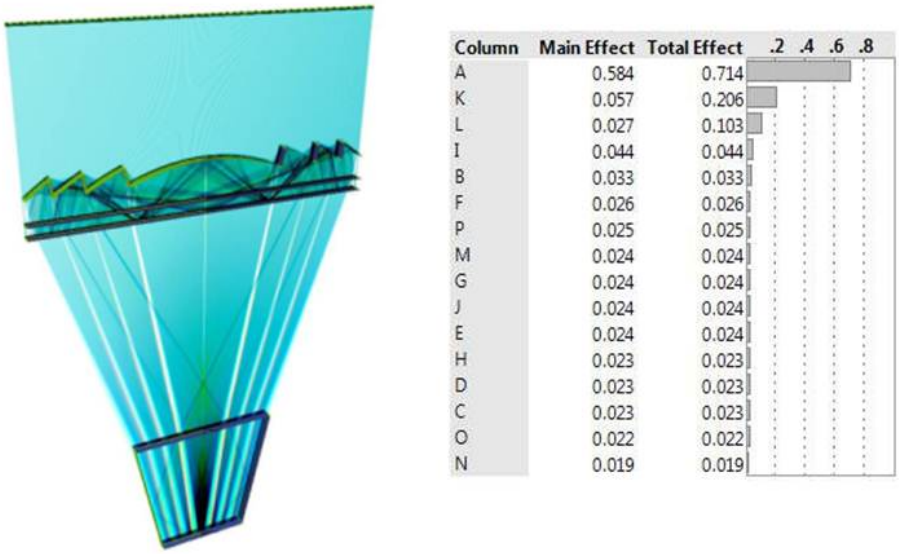

Figure 2.13: Sensitive analysis performed by "MORGAN SOLAR INC." through MSOS software [6].

To measure and predict some of the most complex variables such as the environmental variables, actual standardized tests are usually carried out over a period of six months to one year. During this period, the studied systems are positioned in a solar tracker with two axes and data of misalignments, meteorological variables, current-voltage curves and data of Direct Normal Irradiance (DNI) are taken. After testing, a data analysis is performed in order to find possible correlations between variables measured and, finally, the results can be extrapolated to different locations to predict specific behaviors of the systems [14]. An example of such characterization is presented in Figure 2.14.

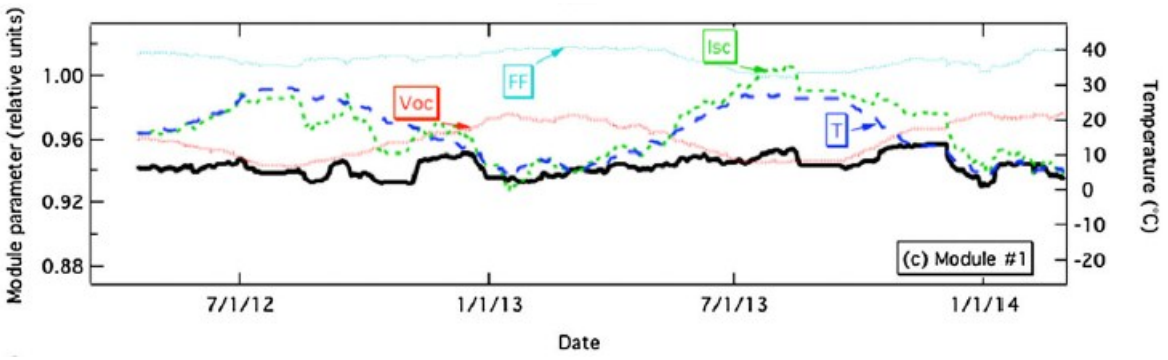

Figure 2.14: Characterization data of a CPV tested where the black line correspond to the performance ratio of the system. [14].

From these analyses it is possible to identify that the environmental variables affecting the behavior of CPV systems are [14] [21]:

- The temperature, not only at the level of the photovoltaic cell. Although cells compromise their efficiency as a function of temperature, must be considered that the lenses suffer deformations that can change their refractive properties. This type of phenomena has not yet been deeply studied.
- The humidity and dust or solid material can cause damage to systems, corrosion, and even affect the passage of light from the lens to the cell by dirt or condensation effects.
- The rainfall can cause structural damage, shorts circuits and indirectly determine the level of sun that receives the system. Therefore, places with high rates of rainfall will present higher index of cloudiness and, furthermore, low levels of Direct Normal Incidence (DNI) required for the system to function properly.

Chapter 3

Proposed Approach

3.1 Introduction

The proposed approach is based on the information recollected from the State of the art and on the experience with a real case during the development of the EAFIT-EPM Solar Car. This project served as an starting point for the research process, highlighting the need to collect practical information to facilitate and improve the CPV systems design process with a theoretical base for a correct performance calculation of the designed system before materialization.

3.2 Research Approach

For the development of the proposal the Action Research Methodology was used. The first cycle of investigation was composed by a Design Inclusive Research where a CPV system was developed according to the state of the art and the analyzed theory, applying the information found to get a design for a practical case defined by specific requirements in order to obtain information about its behavior and compare the theoretical calculations with the real performance of the module.

The next cycle of the research consisted on the analysis the information recollected of the implementation of the CPV system designed in first cycle to complement the theoretical information and finally develop the proposed methodical approach. Figure 3.1 describes the used research methodology [2].

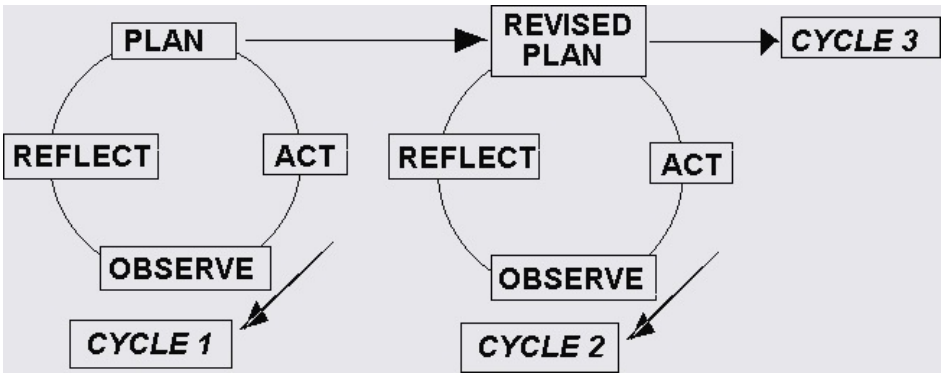

Figure 3.1: Graphical description of the research methodology. [2]

3.3 First Cycle: Design Inclusive Research

A CPV system was developed to be used in the World Solar Challenge 2015 (WSC). Theoretical calculation was carried out with Equation 3.1 [1] in order to describe the behavior of the system and predict its energy production.

$$E = (A_c * S * R * \eta_c * \eta_{op} * \eta_s * N_{CPV} * t_{CPV}) \tag{3.1}$$

For the basic calculation of the potential theoretical energy of CPV systems E [J], the values of the most important parameters are operated, such as A_c = photovoltaic area [m^2], S = number of suns or concentration factor [no units], R = solar radiation [W/m^2], and efficiencies of the components [no units], η_c = cell efficiency, η_{ot} = optical efficiency, η_s = system efficiency, such as electrical components, N_{CPV} = quantity of CPVs [no units] and t_{CPV} = time of use of the system [s] [1].

The CPV system was designed with 60 CPVs, triple-junction cells of 5,5x5,5 mm^2 of 42% of efficiency, concentrator factor of 437,2 suns, Fresnel lenses of acrylic (PMMA) of 115x115 mm^2 and 180 mm of focal length and optical efficiency of 92% approx., as it is presented in Figure 3.2. The efficiency of the system was calculated around 90% approximately.

Figure 3.2: CPV module designed and developed.

For the design and manufacture of the system, tools, such as a laser aligner for Fresnel lenses were manufactured and the interface element was designed to be rigid and lightweight, as it is shown in Figure 3.3. The geometry was based on two functional modules with tray form where the photovoltaic cells were manually assembled.

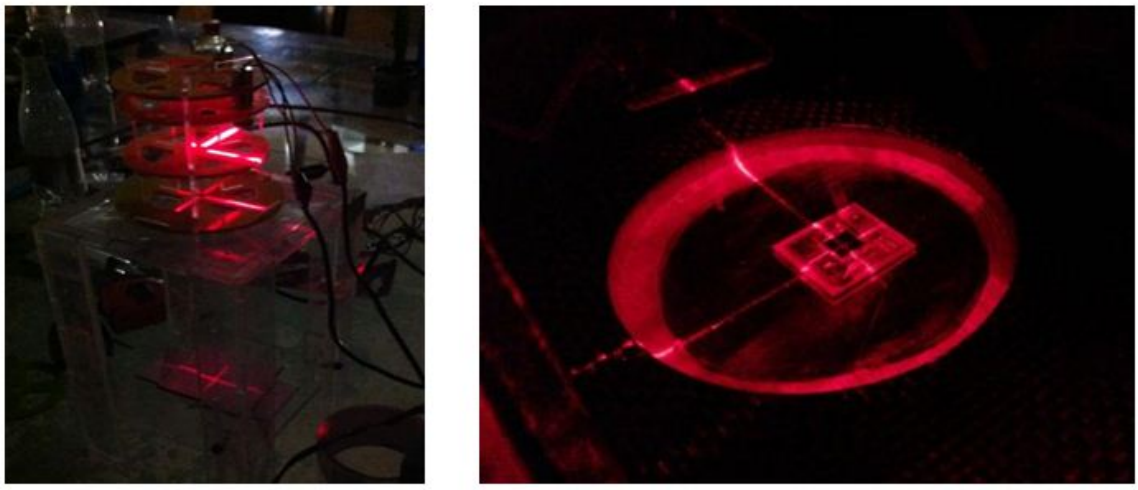

Figure 3.3: Laser aligner for Photovoltaic cells and Fresnel lenses developed.

According to Equation 3.1, the power production of the system was calculated excluding the time and the result suggests 276 Watts of power including the data of design mentioned before. However, the real power measured was 110 Watts, 40% less than the theoretical prediction.

After testing the designed CPV system it was concluded that since the high-energy production comes from the integrated work of all cell, the proper alignment of each one is fundamental to improve the performance of the system. For a specific purpose, not only a correct assembly and alignment process is necessary, but also the design of an interface element capable of keeping this alignment

condition is required. Thus, the rigidity is the most important property needed for the interface element for CPV systems.

The theoretical model of Equation 3.1 does not include factors such as temperature and deformations effects. Also, the solar radiation factor should be delimited only for the Direct Normal Irradiance (DNI) that is the real light component used by the CPV systems. However, DNI can vary drastically with time, so that this function in terms of energy is assumed for constant DNI or an average during used time. For the immediate verification of the error calculation, the power can be a more useful value because it is measured in a specific instant with the real value of DNI.

The improvement of prediction methods and also the development of a method to obtain a best performance of CPV systems are evident. For this reason the methodical process is proposed in the next section.

3.4 Second Cycle: Proposed Methodical Approach

The variables identified through the state of the art and the observation of the CPV system designed for the first cycle can be separated in three groups:

1. Component variables: considering the cell efficiency, the lens efficiency and the interaction between the cell-lens integration. Efficiencies of the components, given by their manufacturers in a datasheet. They represent an initial value to approximate the real performance of a CPV system but, due to the interaction between these elements, they can present a different behavior with the theoretical properties of each component separately. It is necessary to understand the impact of this interaction in the energy production and finally in the real performance of the system.
2. Geometrical variables: which are composed by three displacements for each axis (x, y, z) and one rotation in relation to the cell-lens integration. This group of variables is determined specifically by the manufacture and assembly process and can be translate into tolerances.
3. External variables or environmental variables: like Solar radiations, work temperature, wind forces, humidity levels and precipitation levels. These variables are obtained from the context or contexts of use and they must be included, since these values have strong influence in the design and manufacture stage and later they have direct impact in the behavior of the CPV system.

With the identified groups of variables, the methodical process of design and integration for CPV systems based on design methodologies is defined. The variables are separated in design stage and the specifics steps of the process try to control each variable. Figure 3.4 shows a conceptual diagram, which simplifies the complete process proposed.

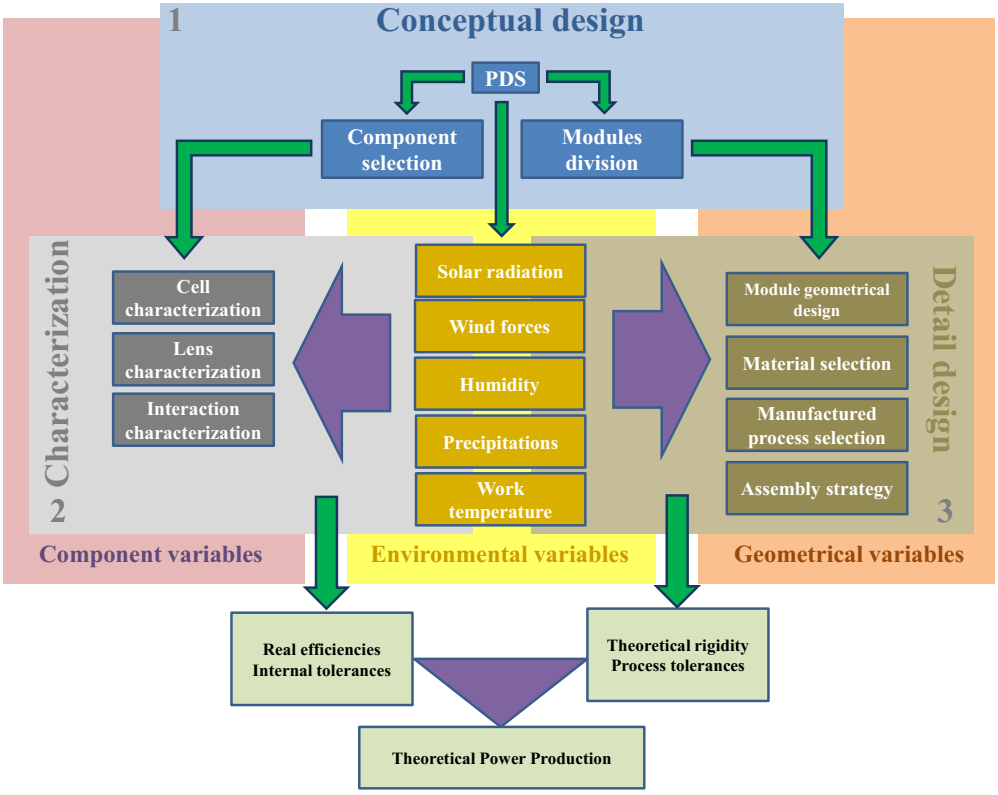

Figure 3.4: Graphic summary of the proposed methodical approach.

The methodical process consists in three main stages: the conceptual design, the characterization and the detail design. The groups of variables mentioned before are implicit in each stage, except the group of environmental variables since these are transversely to the whole process, as it is exposed in the Figure 3.4.

In this way, with the characterization stage in co-analysis with the environmental variables, the real efficiency of the lens-cell interaction, called performance index (PI), is achieved depending on the internal tolerances of this interaction described in the second group of variables. On the other hand, the detail design stage, considering the environmental variables, allows to get the deformation tolerances of the system to keep an energy production limit in determined use conditions, and the tolerances of the process of manufacture and assembly which must be compared with the internal tolerances of the system, in order to determine the energy production that can be reached by process limits and predict a real performance of the designed system. Therefore, the context of use is not just included in the environmental variables but it is also included the context of development and production.

Figure 3.5 presents the flux of the proposed process along with the results of the stages. This can be an iterative process that can return to any stage at any time.

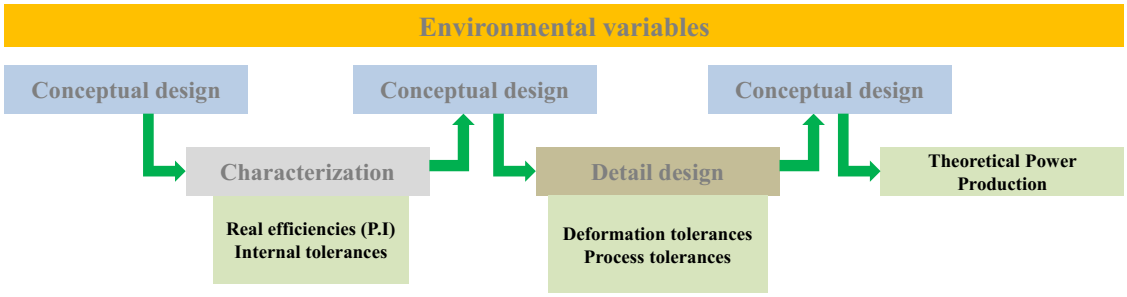

Figure 3.5: proposed flux for the implementation of the methodical process.

3.4.1 Conceptual Design

This stage transforms the requirements of the system in a basic conceptual design considering the main elements of a CPV system, the optical element and the photovoltaic element.

3.4.1.1 Product Design Specifications

The conceptual design begins with the definition of a Product Design Specification (PDS), according to Pugh [23], where he identified 32 basic elements that can be specified, in order to get the better possible description of the requirements of any product and generates a more complete concept that satisfies all the needs for which it was created.

In this case, the PDS can be reduced to the next basic specifications:

- **Performance:** this parameter describes the energy requirements of the system, and it can be expressed as power in Watts or as energy in Watts per unit of time. It is the most important requirement because is the value that can be reached with the design process.
- **Size:** in some cases, the space available for the system can be limited in terms of either area or volume, even in different moments of the use of the system, for example, there can be a limitation for the storage space to transport the system.
- **Working environments:** the contexts of use of the system must be described in terms of variables that have direct relation with the energy production. In this way, the main environmental variables are solar radiation, working temperature, wind forces, humidity levels and

precipitation levels. These conditions can suggest the use of heat dissipater in the cell, the necessary rigidity for the system alignments, possible materials for the interface element and duty or water conditions that can affect the performance of the system and cause damage. This could be prevented with additional elements that guarantee some levels of Index of Protection (IP) according to the international regulation IEC 60529.

3.4.1.2 Component selection

In this step, the general components must be selected according to the PDS. First, it is recommended to select the photovoltaic cell because there is less offer and variation for these elements in the market and they usually have higher costs. These components determine other considerations for the rest of elements, the photovoltaic cells for CPV systems are usually small cells based on photovoltaic materials besides Silicon, which leverage more wavelengths of the light, managing to reach efficiency levels up to 40 %. This efficiency is used in relation to the cell area and the concentrator factor to calculate a first theoretical power production. Therefore, their selection is determined mainly by the energy requirements in the PDS; as it is shown in Figure 3.6 [29].

Sun Concentration	I_{sc} [A]	V_{oc} [V]	I_{MPP} [A]	V_{MPP} [V]	P_{MPP} [W_{MPP}]	FF [%]	ŋ [%]
Version MC/Air Grid optimized for medium concentration + Antireflective Coating adapted to air							
X 250	1,16	3,07	1,14	2,82	3,21	90,1%	42,0
X 500	2,33	3,11	2,29	2,79	6,40	88,3%	41,9
X 1000	4,68	3,13	4,57	2,70	12,33	84,2%	40,4
Version MC/Glass Grid optimized for medium concentration + Antireflective Coating adapted to glass							
X 250	1,15	3,07	1,13	2,81	3,18	90,1%	41,7
X 500	2,31	3,10	2,27	2,80	6,35	88,7%	41,6
X 1000	4,61	3,13	4,52	2,71	12,24	84,8%	40,1

Figure 3.6: Datasheet of a triple-junction photovoltaic cell manufactured by "AZUR SPACE" [29].

Each manufacturer describes the behavior of the cells in terms of power production with standards of solar irradiation of 1000 W/m^2. The typical areas of these cells are 10mm x 10mm, 5 mm x 5mm or less because while smaller the cell, higher concentrator factors can be obtained with smaller optics elements.

With the photovoltaic cell defined, the next step is to define the Fresnel lens. The first consideration is the concentrator factor, which determines the lens area to get a specific energy production. Then, there are other important aspects like the optical efficiency, the material, grooves density, the

transmittance, etc. Some of these aspects are presented in Figure 3.7 [10]. Fresnel lens can be designed specifically for solar energy applications, but the most common and cheapest lenses are for optical applications, which are not highly efficient compared to the lenses designed for solar applications. For CPV systems, it is recommended to use non-imaging Fresnel lens with less grooves density [30]. Also, another way to determinate the lens efficiency is the F number (focal length/diameter), due to, a lens with low diameter and long focal length is suggested according to the curve in Figure 3.7 [5]. Finally, the efficiencies of these two components, cells and lenses, are the first real approach to the efficiency of the CPV system, and Equation 3.1 can be used as a first approach for energy calculation.

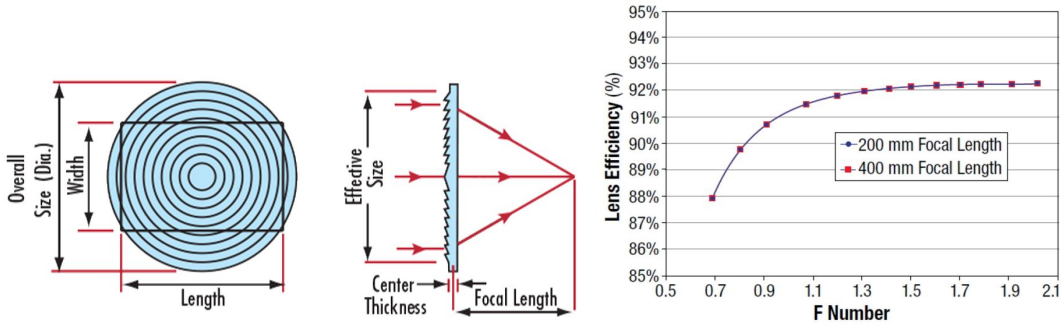

Figure 3.7: Main characteristics of a Fresnel lens. [10][5].

3.4.1.3 Module Division

To generate functional modules of CPVs, first, it is necessary to determine the quantity of the individual CPVs that will be used to integrate the whole system. This number depends on the energy requirements described in the PDS. In this way, the number of CPVs is obtained dividing the needed power between the maximum power of a CPV, as it is shown in the Equation 3.2.

$$N_{CPV} = \frac{W_{needed}}{W_{mpp}} \tag{3.2}$$

Typically, the CPV systems are separated in functional modules and this division allows building units perfectly functional with the possibility to scale them integrating various modules to conform bigger systems in order to generate more energy.

Additionally, requirements of size related with storage dimensions or deployment dimensions can limit the minimum functional module size, the number of functional modules or, even, the number of CPVs, also limited by the available area for lenses. These limitations are represented in Equations 3.3 and 3.4.

$$N_{CPV} = \frac{Deployment\ area}{Lens\ area} \tag{3.3}$$

$$N_{Modulos} = \frac{Deployment\ area}{Storage\ area} \tag{3.4}$$

3.4.2 Characterization

This stage is oriented to test the real behavior of the selected components under an approach of the environmental variables in order to get a more exact prediction of the expected power. Therefore, it is necessary to get some samples of the main elements of the CPV system. Through the Performance Index (PI) a conceptual coefficient that can be operated in the energy calculation is obtained.

3.4.2.1 Cell Characterization

This process allows checking the behavior of the cells under real or simulated work conditions having the data of performance from the manufacturers as starting point. In this way, it is possible to adapt the efficiency of the cells through the Equation 3.5, where η is the percentage efficiency; Pm is the real power obtained from the cell; E is the sun irradiation and Ac is the photovoltaic area.

$$\eta = \frac{p_m}{E * A_c} \tag{3.5}$$

3.4.2.2 Lens characterization

With the selected lens, it is necessary to analyze its real behavior standing between the light and the photovoltaic cell. For this reason, it is important to know its response in terms of temperature variation and deformations, humidity, wind forces, dust and rain. Under these conditions, the chromatic aberrations or differential focal points, performance to different wavelengths and mainly the optical efficiency or energy that crosses by the lens, can be determined through tests of transmittance. Many of these tests can be carried out in simulation software and real tests with controlled environmental conditions, yielding properties as it is presented in Figure 3.8.

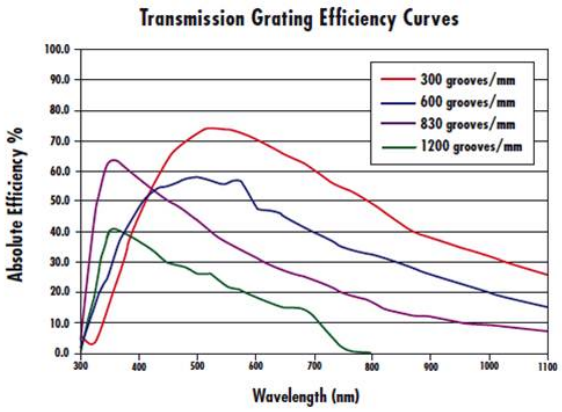

Figure 3.8: Typical Fresnel lens graphic by "EDMUND OPTICS INC" [10].

3.4.2.3 Interaction characterization

This characterization allows getting a PI in terms of power, according with the real behavior of the integration between lens-cell. The main measure is the power of a cell in function of the displacements in each axis (x, y, z). For each position in each axis, there will be a corresponding power value and there will be a value or range of maximum power production as it is shown in Figure 3.9. This process determines the sensibility of the system in function of the alignment errors. In this way, it is possible to select the interval of positions that keeps the power level of the whole system within the energy or power requirements, getting a set of maximum internal tolerances for each measured axis.

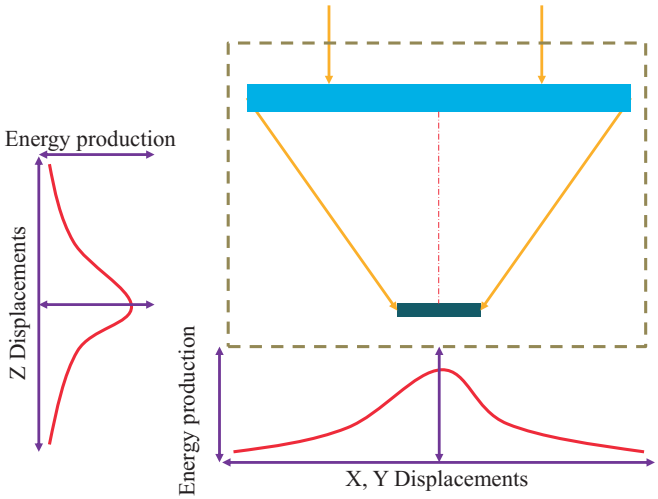

Figure 3.9: Graphics of the CPV energy production in function of the displacement in each axis.

Finally, to correct the error of the theoretical power and the real power, a Performance Index, PI, is calculated according to the Equation 3.6.

$$PI = \frac{Real\ power}{Theoretical\ power} \tag{3.6}$$

3.4.3 Detail Design

The final stage of the process is oriented to design an appropriate interface element satisfying the requirements presented in the PDS through the correct inclusion and control of the different variables that affect the systems. For the design of the interface element, environmental conditions focused on the need of a rigidity level to keep the manufacture and assembly conditions are taken into account. Essentially, the geometry of the elements, the material and the manufacturing process define the rigidity. For this reason, in this stage the different steps could be worked in parallel.

Looking forward to simplify the designs and improve the control of the different parameters, some design guidelines to generate a more functional concept are considered. These guidelines are minimum quantity of parts, minimum quantity of mobile parts and auto-alignment assemblies.

3.4.3.1 Module geometrical design

The geometry of the modules refers to the dimensions and the type of profiles and geometrical elements

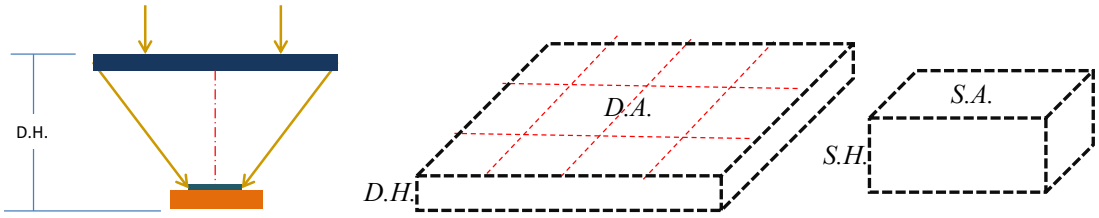

Figure 3.10: Volumes of deployment and storage of a CPV system.

- ***Deployment Height (D.H.):*** *Focal length lens + lens thickness + base thickness.*
- ***Storage Area (S.A.):*** *Deployment area / modules number.*

- ***For Storage Height (S.H.)**, two cases may occur:* By stacking the modules one on another, with its own height fixed.

  - *Storage Height (S.H.) = Deployment Height * modules number*

  Or in case of restrictions of space and the height storage is less than the height of stacking. For this case, it is necessary to develop a way to vary the height of modules for storage times without affecting its functionality for deployment times as it is shown in Figure 3.11.

  - *Storage Height (S.H.) < Deployment Height * modules number.*

Figure 3.11: Cross section of CPV modules with variable height.

The profiles, cross sections or geometrical elements determine the geometric rigidity in presence of forces or loads. The main loads, which the modules will be subjected, are its weight and wind forces, so the rigidity of the modules must overcome them. The first load can be approximated by adding the individual weight of each component, and then this value has to be corrected with the calculation of the weight of the interface element.

The wind forces can be obtained from the maximum wind speed registered in the context of use, through Equation 3.7, where ρ = Air density, $D.A.$ = Deployment area, Cd = Coefficient of aerodynamic drag ($Cd = 2$ for rectangular shapes) and $W.Speed$ = Maximum wind speed.

$$WindF = \frac{1}{2} * \rho * D.A. * Cd * W.Speed^2 \tag{3.7}$$

For practical purposes, the analysis can suppose a configuration of maximum load as it is shown in Figure 3.12(a) where the modules are rigidly supported in its shorter side and there is a distributed load in the top of them. This configuration can be solved with the Equation 3.8 to calculate the rigidity of a beam in terms of δmax (maximum deflection in length units), w = distributed load, L = length, E = rigidity module of material and I = inertia given by used geometric elements. In this way, a maximum deflection value can be calculated according to the internal tolerances of the system from the interaction characterization step, as it is shown in Figure 3.12(b). With the resultant inertia,

a specific geometrical profile or cross section can be designed. The material for E is specified in the next step.

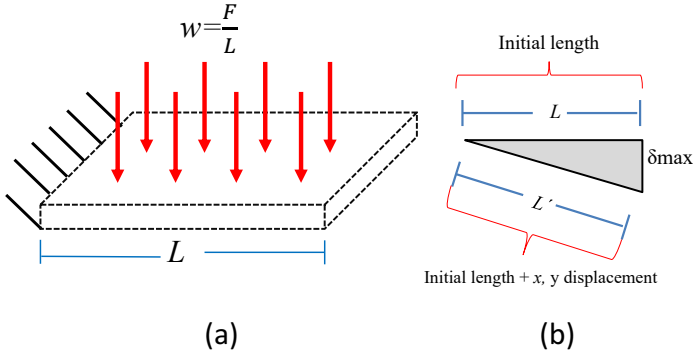

Figure 3.12: (a) Configuration for the module analysis, and (b) diagram of displacement errors presented by deflections.

$$I \geq \frac{-w * L^4}{8 * \delta max * E} \tag{3.8}$$

The deflection of the module represents a direct z axis displacement, nevertheless, there are x and y axes displacements resulting from this deflection, the level of these displacements can be known through Equation 3.9.

$$x, y\ displacements = (\frac{length}{sin(tan^{-1}(\frac{\delta max}{length})}) - length \tag{3.9}$$

3.4.3.2 Material Selection

This step complements the last step for the expected rigidity levels. Taking into account the temperature, humidity and precipitation levels, it is possible to propose some materials adapted to these environmental conditions with specific E values. Then, the Equation 3.10 is used to determine a rigidity module for the previously calculated inertia, and, finally, the correct material in concordance with the requirements is selected.

$$E = \frac{-w * L^4}{8 * \delta max * I} \tag{3.10}$$

3.4.3.3 Manufacture Process Selection

The process of manufacture depends on the manufacture capabilities, the selected material and the geometry, as it is presented in Figure 3.13. However, not only the environmental conditions should be

considered, but also the internal tolerances from the characterization stage, in order to guarantee the needed tolerances for the components in relation to the positions of the lenses and cells.

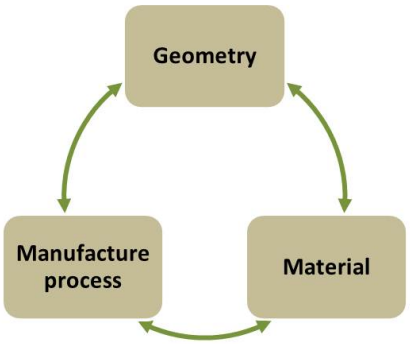

Figure 3.13: Iterative process for the definition of geometry-material-manufacture process.

3.4.3.4 Assembly Strategy

This step is strongly related with the manufacture process considering that this is a method focused on the lens and cell assembly. For this step, it is necessary to review the internal tolerances of the system and the process of manufacture, determining the appropriate method for assembly:

- Assembly centered in the interface element, as it is shown in Figure 3.14: assembling many cells in one-step through molds, jigs or some tools developed. For this procedure, it is necessary to ensure that the manufacture process, to make the assembly tools, has tolerances inside the range of internal tolerances of the system.

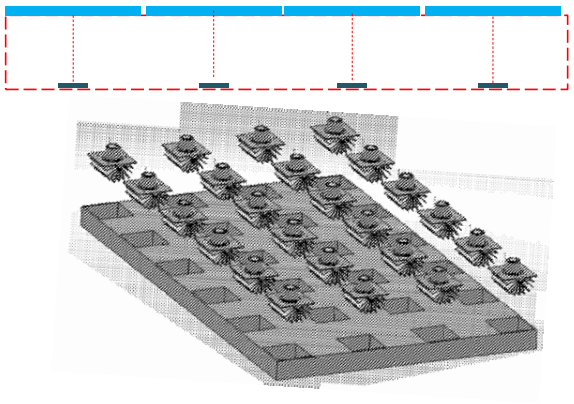

Figure 3.14: Assembly centered in the interface element.

- Assembly centered in photovoltaic element, as it is shown in Figure 3.15: assembling the cells or the lenses one by one to ensure the perfect alignment between lenses and cells. This method is recommended when the process tolerances are outside the system tolerances or when there is not enough control of the process tolerances.

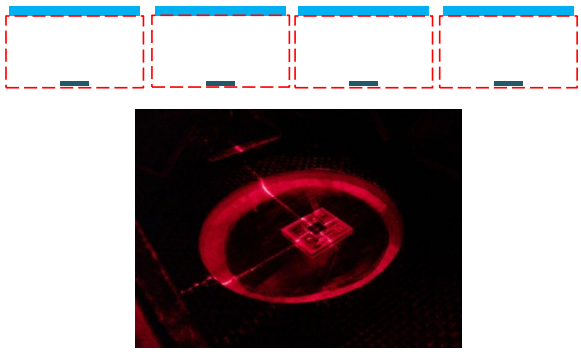

Figure 3.15: Assembly centered in photovoltaic element.

3.4.3.5 Theoretical Energy Production

Finally, it is possible to approach a theoretical adjusted power (TP). Knowing all the details of the design of the interface element and the measured *PI*, it is possible to calculate the *Tolerances Ratio (TR)*, between the tolerances needed for the system or the range of misalignments that do not affect the needed power, and the tolerance levels of the process plus the displacements by deflection using Equation 3.11.

$$TR = \frac{Internal\ tolerances}{Process\ tolerances + deflections\ tolerances} \leq 1 \tag{3.11}$$

The *TR* factor is integrated to the power calculation and it must be less or equal to 1. In this way, when the minimum level of process tolerances is higher than the maximum level allowed by the internal tolerances of the system, the *Theoretical Power (TP)* will be reduced by these factors. When process and deflection tolerances are less than system internal tolerances, the TR value will be equal to 1. The Theoretical Power (TP) can be calculated using Equation 3.12, where the *PI* summarizes the efficiency factors of the cells and lenses, the other factors are: $Acell$ = cell area, $Nsun$ = number of suns or concentration factor, DNI = Direct Normal Irradiation measured or calculated, ηsys = efficiency of electrical components of the system and $Ncpv$ = number of used CPVs. The TR factor is divided in two parts: tolerances for x and y axes, which may be equivalent, and tolerances for z axis. All these tolerances are affected by the tolerances of the manufacture and assembly processes of the

parts related with the position of the cells and lenses and by the maximum deflection levels, as it was presented in the Module geometrical design step.

$$TP = (A_{cell} * N_{sun} * DNI * PI * \eta_{sys} * N_{CPV}) * (TR_{x,y}) * (TR_z) \tag{3.12}$$

For determining a correct DNI in the power calculation, it is recommended to sense the real direct light components through radiation sensors with filters for diffuse radiation. Even so, there are mathematical models to determine an approximate value of the proportion for the DNI from the total solar radiation, as it is shown in Equation 3.13 [24], where AM=air mass factor which works like diffuser for the sun light and is defined by the Zenith angle θ (90 ° - Sun altitude) in Equation 3.14 [24].

$$DNI = Total\ Solar\ Radiation * 0,7^{AM^{0,678}} \tag{3.13}$$

$$AM = \frac{1}{cos(\theta)} \tag{3.14}$$

Chapter 4

Experiment

4.1 Introduction

The experimental part is divided in two focuses of analysis, the first one related to the cell-lens interaction, in order to characterize the behavior of some combinations of cell-lens in function of the components alignment, under real conditions of use, and to obtain a relation of internal tolerances and Performance Indexes (PI).

The second focus is related to the implementation and understanding of the proposed process, using the CPV system designed in the first cycle to verify its data through the equations of the methodical process and compare the theoretical production of recalculated power with the measured power. Finally, the methodical process was implemented with a group of engineers to solve a theoretical case with parameters and initial requirements defined as the required energy production, the Performance Index of the components used, the materials and manufacturing processes allowed, tolerances, environmental conditions, etc. The whole experiment process can be related in two specific fundamentals of the methodical process proposed as it is shown in Figure 4.1.

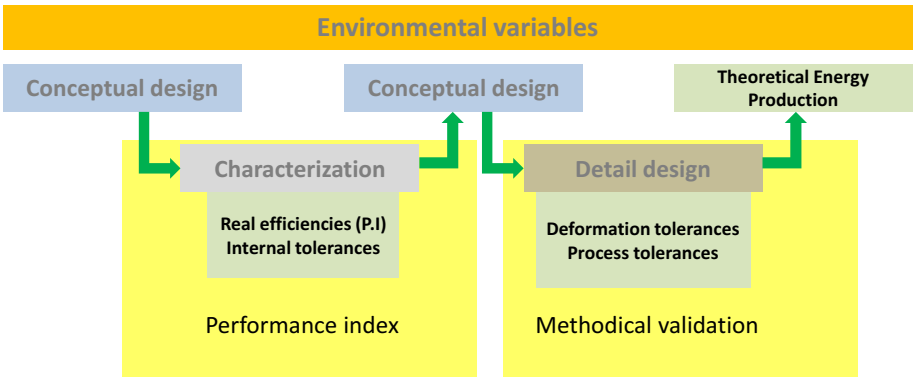

Figure 4.1: Focuses of experimentation for the methodical process proposed.

4.2 Performance Index and Internal Tolerances

The objective of this first experimental part consists in measuring the change of power registered in a solar cell as a function of movement in axes x, y and z.

Some lens manufacturers, like Fresnel Factory [5], suggest a solar cell position in such a way that the light passing through the lens covers the entire cell, inscribing the light spot perfectly over the area of the cell as it is shown in Figure 4.2. In this way the concentration factor is the difference between the lens and cell areas, however, the maximum power production could be in different cell positions.

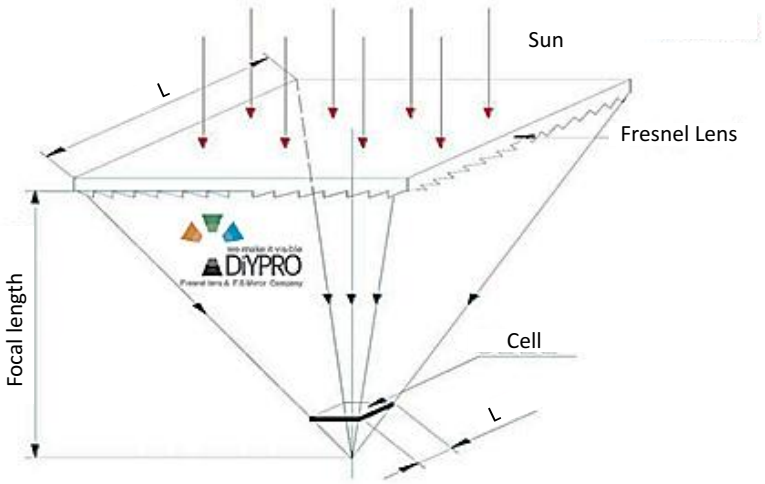

Figure 4.2: Typical CPV configuration for concentration factor. [5]

The Figure 4.3 describes graphically a theoretical position of the solar cell (represented by the black square) with respect to the light spot formed through the Fresnel lens (represented by the yellow circle).

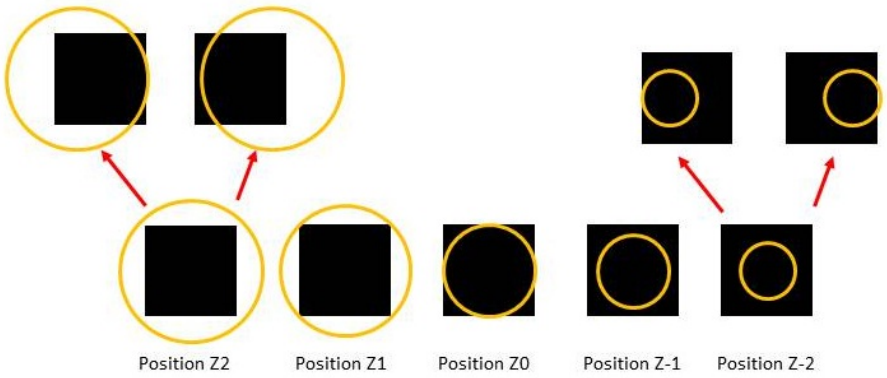

Figure 4.3: Representation of the light spot on the solar cell for different misalignments.

With this test, it is expected to obtain a bell graph showing a maximum point of power in relation with a specific position, achieving to identify an optimal position of the solar cell and its permissible misalignment tolerances, as it is observed in Figure 4.4. Then, this power can be compared to the Theoretical Power (TP) calculated with manufacturers information and, then, obtain the Performance Index (PI).

4.2.1 Test description

The interaction test is performed with one type of triple junction photovoltaic cell of 5,5x5,5 mm^2 provided by Azur Space [29]. The cell used for the design of the CPV system for The World Solar Challenge 2015. Two types of Fresnel lenses are used: a circular lens with 70mm of focal length and a diameter of 260 mm; and a square lens of 182 mm of focal length and 115 mm of side, both provided by Fresnel Factory [5]. These components are shown in Figure 4.5.

For the selection of the cell position in z axis, in order to generate a specific light spot diameter, it is possible to represent the light path in triangle shape knowing the lens length or the lens diameter used, and its focal length. Then, the cell is positioned represented by an horizontal line or plane cutting the light triangle allowing to know the diameter of the light spot projected on the top. Finally, the focal length or the distance of the solar cell regarding the lens is obtained through similar triangles ratio using Equation 4.1 where $N.F.L.$ is the Nominal Focal Length of the lens, $\phi Spot$ is the Light Spot Diameter and $\phi Lens$ is the Lens Diameter. This process is represented in Figure 4.6.

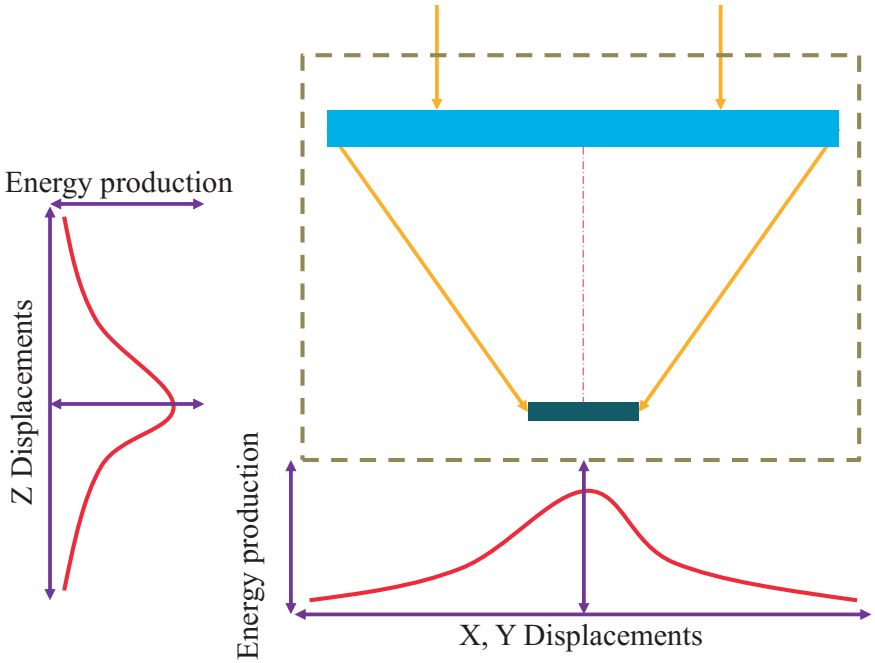

Figure 4.4: Expected curves of interaction characterization step.

$$Focal\ Length = N.F.L - (\frac{N.F.L. * (\frac{\phi Spot}{2})}{(\frac{\phi Lens}{2})}) \tag{4.1}$$

4.2.1.1 Test 1

A first characterization test is done with a module of six places, for six combinations lens-cell, in order to accelerate the process and to have more repetitions at the same time. This module works just with the circular lenses, allowing to change alignment conditions in each cell-lens combination and conserving the same environmental conditions. This module includes a visual aligner which allows to position it with respect to the sun. Data of power measures, solar irradiation and temperature of the CPVs are sensed. The module is shown in Figure 4.7.

The modules are divided in two rows of three cells each one, the row 1 uses three solar cells with theoretical efficiency of 43% and allows horizontal movements for simulate misalignment in x axis. The row 2 uses three solar cells with theoretical efficiency of 42.1% and allows vertical movements for simulating misalignment in y axis. For the misalignment control, the displacements of all the cells in both axis is the same for each sub test, with a range from -5 mm to 5 mm. The Figure 4.8 summarizes the allowed movements.

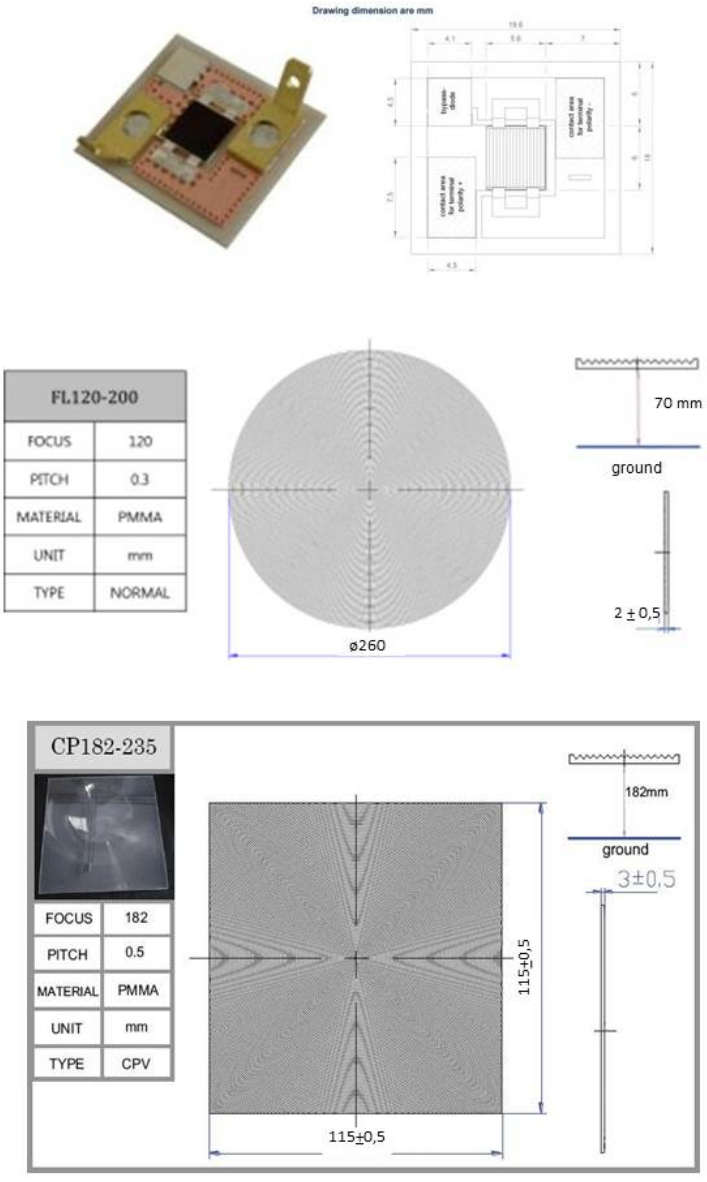

Figure 4.5: Specifications of cells and lenses used. [29][5]

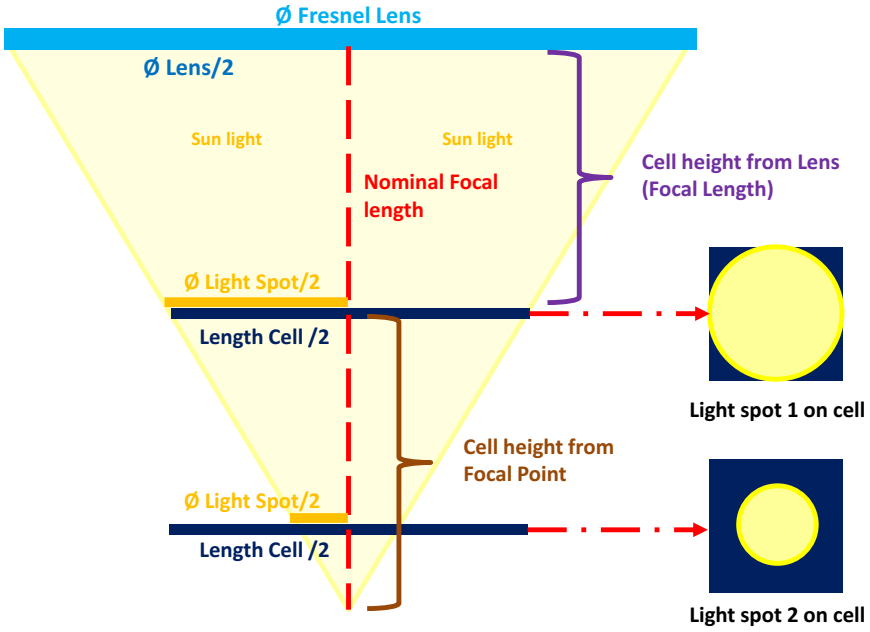

Figure 4.6: Graphical representation of the similar triangle ratio for selection of focal length.

Figure 4.7: Test module for six cell-lens combinations.

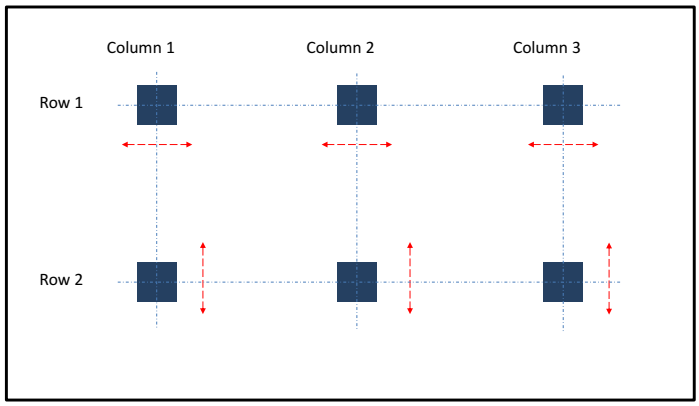

Figure 4.8: Solar cells configuration array for misalignment test.

The rows have the same three heights of cells or focal lengths, one for each column. Taking a focal length of 67,72 mm as reference (theoretical length which the light spot is inscribed inside the cell area for circular lenses), the focal length of the cells in the column 1 is the reference 67,72 mm, the second one is 1 mm over the reference (68,86 mm), and the third one is 2 mm over the reference, reaching the nominal focal length of the lens (70 mm) as it is shown in Figure 4.9.

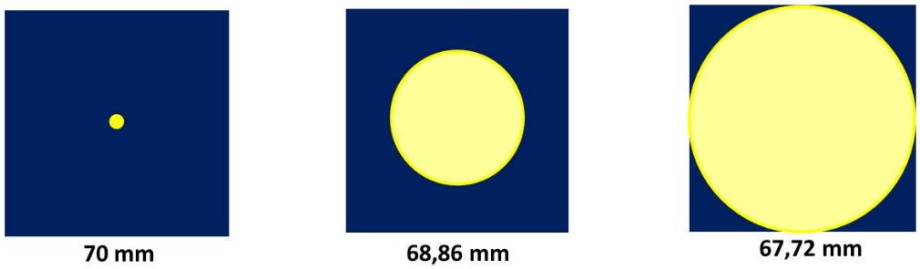

Figure 4.9: Light spot representation for different focal lengths.

Data of short circuit current, open circuit voltage and solar radiation are taken simultaneously through multimeters and a pyranometer. Each sub test is performed every two minutes to take five samples, each data is taken every 30 seconds and get average values for the calculation of the power form factor, multiplying the current and voltage values, the data is summarized in Table 4.1.

Table 4.1: Table test 1.

Day 1-Plane alignment							
Time (min)	Cell 1	Cell 2	Cell 3	Cell 4	Cell 5	Cell 6	S.R.(W/m^2)
	P(W)	P(W)	P(W)	P(W)	P(W)	P(W)	
0,5							
1							
1,5							
2							
2,5							

4.2.1.2 Test 2

The second test is performed with a module developed to improve the control of the movements in each axis of the solar cell. The module is designed to use the two types of Fresnel lenses (circular and square) and it includes a mobile base with a total displacement in the z axis of 230 mm away from the Fresnel lens to articulate the focal length for each lens used. The support of the solar cell allows independent movements in each axis (x, y, z) with a range from -3,5mm to 3,5mm, this support is of aluminum and works like heat sink. Finally, a rotating base is included with the visual aligner used for test 1 to position the module with the sun. The module used for this test is shown in Figure 4.10.

Figure 4.10: Test module for single lens cell combination misalignment.

For this test, three solar cells with 43% of theoretical efficiency are used, two circular Fresnel lenses and two square Fresnel lenses. The cells will be moved or misaligned in x axis from the light spot in a range of -3 mm to 3 mm with steps of 1 mm, being 0 mm the alignment between the light spot and the cell center.

For the movements in z axis, the similar triangles ratio was used with each lens for the determination of the initial focal length for the test (theoretical length which the light spot is inscribed inside the cell area for circular lenses). In the case of the circular lens, the test module reduces its diameter from 260 mm to 175 mm, conserving the focal length of 70 mm. According to this, the initial focal length is 67,8 mm. From this reference, 4 focal lengths are measured, with steps of 1 mm, corresponding to 68,9 mm, 70 mm, 71,1 mm and 72,2 mm.

The square lens has a nominal focal length of 182 mm and side of 115 mm, resulting in an initial focal length of 173,3 mm (theoretical length which the light spot is inscribed inside the cell area for circular lenses). The next focal length will be 176,3 mm, 175,3 mm, 174,3 mm, 172,3 mm, 171,3 mm, 170,3 mm. The focal lengths of both lenses were associated with numbers beginning from 0 to -4 as it is shown in Tables 4.2 and 4.3.

Table 4.2: Focal Lengths for Circular Lens

Focal Lengths for Circular Lens	
N Position Z	Z Height (Focal length)
0	67,8 mm
-1	68,9 mm
-2	70 mm
-3	71,1 mm
-4	72,2 mm

Table 4.3: Focal Lengths for Square Lens

Focal Lengths for Square Lens	
N Position Z	Z Height (Focal length)
3	170,3 mm
2	171,3 mm
1	172,3 mm
0	173,3 mm
-1	174,3 mm
-2	175,3 mm
-3	176,3 mm

Finally, data of open circuit voltage, short circuit current and solar radiation are taken. Power/Solar Radiation ($P/S.R.$) factor results of the division between the Power measured and the solar radiation, and represents a process of normalization, suppressing the effect of a mayor or minor solar radiation in the measure time. This process allows an appropriate comparison of the results. The results of x displacements are grouped for each z position, obtaining 5 tables of results with 7 positions each one as it is represented in Table 4.4.

Table 4.4: Table power test for a Z position in function of X positions.

N Position Z (F.L.)				
N Position X	X Positions (mm)	P (W)	S.R. (W/m^2)	P/S.R.
3	3 mm			
2	2 mm			
1	1 mm			
0	0 mm			
-1	-1 mm			
-2	-2 mm			
-3	-3 mm			

4.2.1.3 Test 3

It is important to know the temperature of the CPV elements because this directly affects the efficiency of the cell and produces deformations in the lens. These effects can be quantified and included in the PI value through efficiency curves as a function of temperature and real power measurements. To do this, the lens-cell combination is tested under real conditions of use, for 10 minute cycles and, information of Power, Solar Radiation, relation between Power and Radiation and Temperature is registered, as it is shown in Table 4.5.

4.3 Theoretical implementation of the process

The second part of the experimentation searches to validate the methodical process, in both its application and understanding, through a practical case based in the information recollected from the design of the CPV system for WSC and a proposed theoretical case.

4.3.1 Practical case: Recalculation of CPV system power for WSC

For the application of the process proposed, the data of the previously developed CPV system were taken to recalculate the theoretical power production and determine the adjustment of the value obtained before. The data of this CPV system is defined in Table 4.6.

Table 4.5: Table temperature test.

Temperature Test				
Time (min)	P (W)	R (W/m^2)	P/S.R.	T (°C)
0,5				
1				
1,5				
2				
2,5				
3				
5				
7				
10				

Due to the specific design and implementation strategy, the analysis should be performed for each module and the theoretical energy production will be the sum of both. Also, the deflection analysis should be made considering the center of the whole deployed system like a fixed ground for each half module because in this part is located the support structure of the real system. The blue prints of the CPV modules of the design are presented in Figure 4.11.

4.3.2 Theoretical Case

A design problem for a solar system together with the methodical process and a series of restrictions is given to a pair of engineers in order to produce a theoretical design and energy production considering the factors included in the process

Brief

A CPV system to energize two cottages of 60 m^2 built in areas of 100 m^2 in rural zone near to Medellín is required.

Initially, both cottages will be energized with the same CPV system but in different times in the month of January. As a reference value, it is known that the average energy consumption of a 50 m^2 - 80 m^2 house is approximately 3,5 KWh/day.

The environmental conditions of the zone are:

- Zenith: $23,6°$
- Solar radiation: 4,5 Kwh/m2

Table 4.6: WSC CPV system data.

Lenses	Square Fresnel lenses of 3 mm thickness, sides of 115 mm x 115 mm, focal length 180 mm, theoretical efficiency 92%
Solar cells	Triple-junction, sides of 5,5 mm x 5,5 mm, theoretical efficiency of 42%
Concentration factor	437
Topology	Tow tray modules of Foam board covered with a layer of Textrim carbon fiber with thickness of 5,5 mm and Fresnel lens array in an profiles aluminum structure type T with 1mm of thickness and 8 mm of height
Maximum deployment dimensions	Length:1975 mm - Width:480 mm - Height:185 mm
Maximum storage dimensions	Length:1035 mm - Width:480 mm - Height:100 mm
Weight	8 Kg
# CPVs	60
Electrical system efficiency	90%
Maximum generated power	110 W to 1088 W/m^2
Average generated power	Approximately 75 W

- Sun hours: 6 h
- Average wind velocity: 28,8 Km/h
- Average temperature: $21,5°$C
- Average air density: 1,16 Kg/m^3
- Average precipitation: 65 mm/month
- Relative humidity: 67%

The system must be able to be transported in an utility car (REF:3W 200) with a loading capacity of 370 Kg, presented in Figure 4.12, since the cottages are 8 Km away.

For the development of the system the follow elements are present:

- **Solar Cell:** Triple-junction of Galio with efficiency of 42%, area of 5,5 mm^2 x 5,5 mm^2 and weight of 2 g, provided by Azur Space.

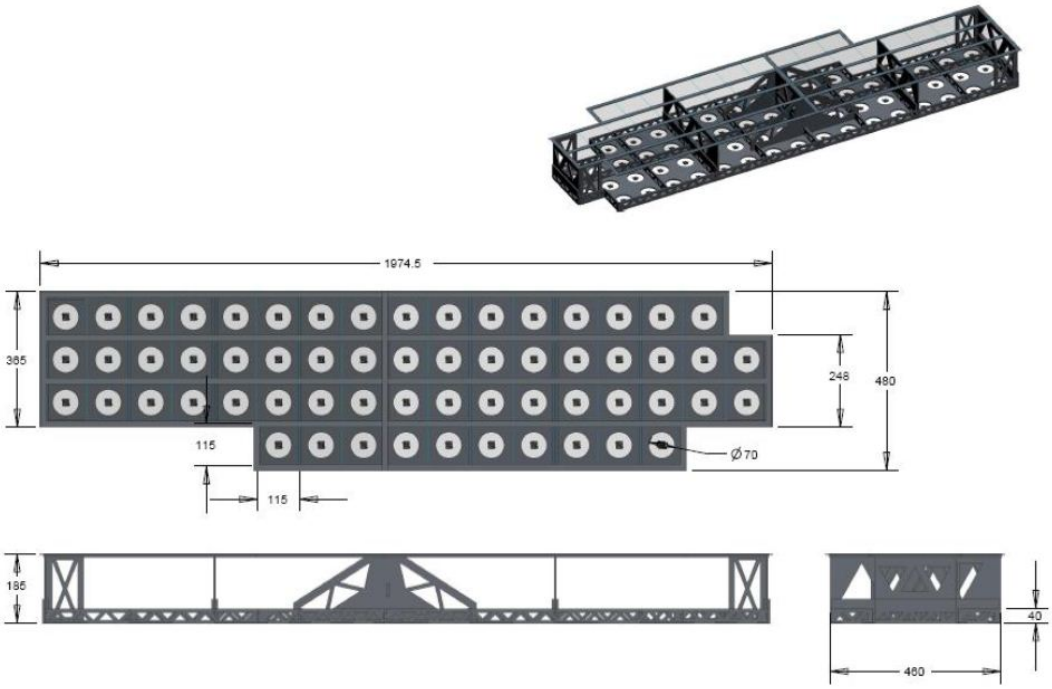

Figure 4.11: WSC CPV module general dimensions in milimeters

Figure 4.12: Available vehicle to transport the CPV system (AKT CARGUERO 3W200)

- **Fresnel lenses:** Lenses of Acrylic with area of 180 mm^2 x 180 mm^2, Focal length of 70 mm and weight of 47 g, provided by Fresnel Factory.

Available materials:

- **Steel 1020:**
  - **Rigidity module (E):** 220 GPa
  - **Density (ρ):** 7850 Kg/m^3
- **Carbon Fiber and Epoxy Resin:**
  - **Rigidity module (E):** 20 MPa
  - **Density (ρ):** 1548 Kg/m^3
  - **Average thickness of each layer (t):** 0,15 mm
  - **thickness for 7 layers (t):** 1,33mm + - 0,4
  - **thickness for 12 layers (t):** 1,77mm + - 0,5
- **MDF:**
  - **Rigidity module (E):** 2,1 GPa
  - **Density (ρ):** 780 Kg/m^3
- **Acrylic:**
  - **Rigidity module (E):** 2,94 GPa
  - **Density (ρ):** 1180 Kg/m^3

Available process:

- **Laser cut:**
  - **Wood (MDF):**cutting error of 0,6 mm.
  - **Acrylic:** Cutting error of 0,4 mm.
  - **Steel:** Cutting error of 0,8 mm.
- **Milling:**
  - **Steel:**Milling error of 0,03 mm - 0,05 mm and error cut for hole of 0,1 mm.
  - **Wood:** Milling error of 0,1 mm - 0,3 mm and error cut for hole of 0,4 mm.

– **Carbon Fiber:** Milling error of 0,1 mm - 0,5 mm and error cut for hole of 0,8 mm.

For this case, the results of the cell-lens interaction characterization step are given to the engineers in Table 4.7 and Table 4.8 and Figure 4.13 and Figure 4.14

Table 4.7: Theoretical characterization values for Z axis (F.L Z=Focal length in Z, C=Short circuit current, V=Open circuit voltage, S.Rad=solar radiation, P=Instantaneous power and P/S.Rad=Instantaneous power divided by Solar radiation).

Characterization Z axis						
N position Z	F.L. Z (mm)	C (A)	V (V)	S. Rad (W/m2)	P (W)	P/S. Rad
-3	71,5	1,22	2,68	1090	3,269	3×10^{-3}
-2	70,5	1,308	2,71	1130	3,545	3.14×10^{-3}
-1	69,5	1,308	2,65	1100	3,466	3.15×10^{-3}
0	68,5	1,25	2,74	1090	3,425	3.14×10^{-3}
1	67,5	1,32	2,71	1066	3,577	3.36×10^{-3}
2	66,5	1,274	2,71	1075	3,452	3.21×10^{-3}
3	65,5	1,25	2,66	1080	3,325	3.08×10^{-3}

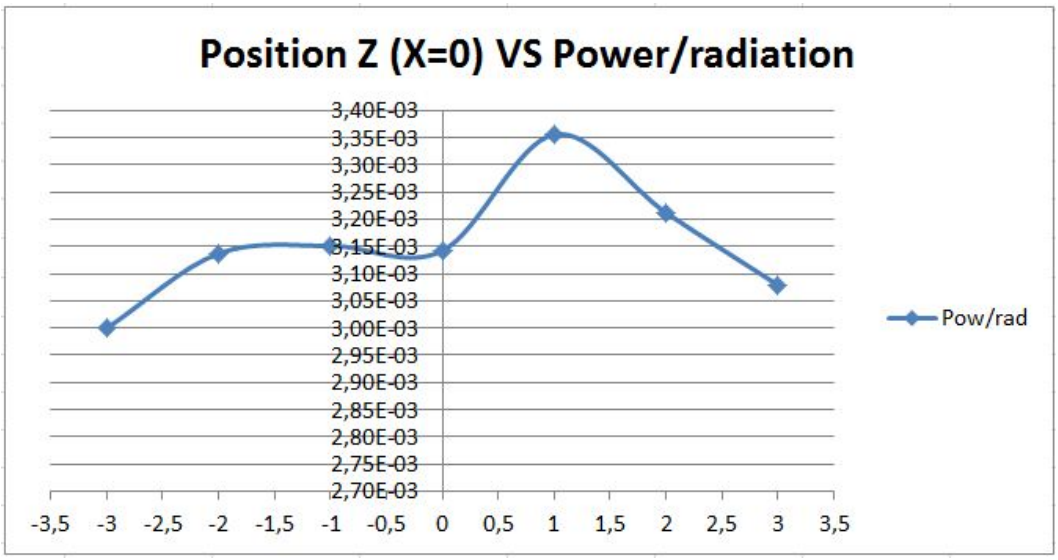

Figure 4.13: Theoretical characterization curve for Z axis in X=0.

Table 4.8: Theoretical characterization values for X,Y axes (C=Short circuit current, V=Open circuit voltage, S.Rad=solar radiation, P=Instantaneous power and P/S.Rad=Instantaneous power divided by Solar radiation)

Characterization X,Y axis						
N position X	Misalignment X (mm)	C (A)	V (V)	S. Rad (W/m2)	P (W)	P/S. Rad
-3	-1,5	1,037	2,6	1020	2,696	2.64×10^{-3}
-2	-1	1,054	2,71	1053	2,856	2.71×10^{-3}
-1	-0,5	1,082	2,68	1047	2,899	2.77×10^{-3}
0	0	1,301	2,720	1055	3,54	3.35×10^{-3}
1	0,5	1,150	2,7	1080	3,105	2.88×10^{-3}
2	1	1,123	2,67	1082	2,998	2.76×10^{-3}
3	1,5	1,049	2,65	1073	2,779	2.59×10^{-3}

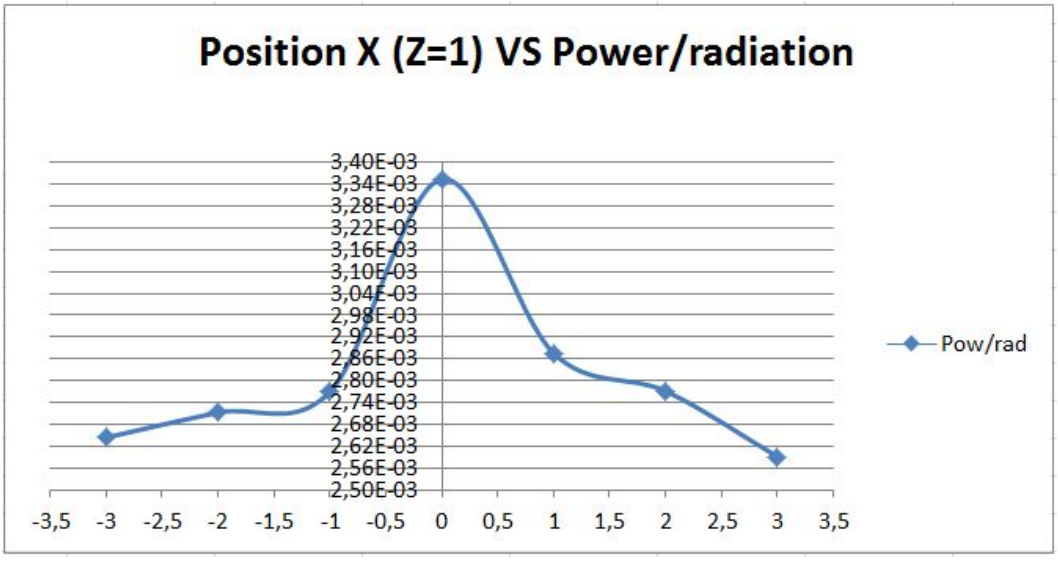

Figure 4.14: Theoretical characterization curve for X,Y axis in Z=1.

Chapter 5

Results

The results and the whole data for each experiment exposed in the last chapter are shown and summarized. Then, results analyses and conclusions are presented.

5.1 Performance Index and Internal Tolerances results

5.1.1 Test 1 results

The first test considers a module of 6 CPVs to test them at the same time in order to carry out a faster test with the same environmental conditions. For each data collection a controlled discrete movement of the axes was done. The set of results is present in Table 5.1.

Table 5.1: Test 1 results set.

Day 1-X,Y(0,0)							
Time (min)	Cell 1	Cell 2	Cell 3	Cell 4	Cell 5	Cell 6	Rad (W/m^2)
	P (W)	P (W)	P (W)	P (W)	P (W)	P (W)	
0	0,465	0,432	0,346	0,423	0,345	0	899
0,5	0,353	0,304	0,203	0,197	1,66	0	901
1	0,445	0,410	0,084	0,415	1,783	0	892,5
1,5	0,452	0,416	0,314	0,408	0,318	0	923
2	0,452	0,405	0,306	0,422	0,317	0	920,5

The strategy was to take a set of data for some discrete positions of the cell, but the control of the components for achieving the movements presented problems due to the materials used and the designed strategy to carry out the movements. Also, some failures in some multimeters were presented impeding the data collection of the whole system. For these reasons, the results of the test 1 were obviated for the data analysis and just the data collected with test 2 and test 3 were used.

5.1.2 Test 2 results

The control system of movements using screws improved the test performance regarding test 1, allowing to take a large amount of data of power in different positions.

5.1.2.1 Circular Fresnel lens

The data of the x displacements obtained was grouped for each Z position of focal length variation. The results are shown in Tables 5.2 to Table 5.6.

Table 5.2: Test 2 results for circular lens in F.L.=Z0

N Position Z0 (F.L. 67,7 mm)				
N Position X	X Positions (mm)	P (W)	S.R. (W/m^2)	P/S.R.
3	3 mm	0,652	1049	6.215×10^{-4}
2	2 mm	0,677	1042	6.497×10^{-4}
1	1 mm	0,688	1052	6.539×10^{-4}
0	0 mm	0,676	1042	6.487×10^{-4}
-1	-1 mm	0,647	1044	6.197×10^{-4}
-2	-2 mm	0,607	1053	5.764×10^{-4}
-3	-3 mm	0,541	1047	5.175×10^{-4}

Table 5.3: Test 2 results for circular lens in F.L.=Z-1

N Position Z-1 (F.L. 68,8 mm)				
N Position X	X Positions (mm)	P (W)	S.R. (W/m^2)	P/S.R.
3	3 mm	0,636	1048	6.068×10^{-4}
2	2 mm	0,761	1059	7.186×10^{-4}
1	1 mm	0,783	1053	7.436×10^{-4}
0	0 mm	0,783	1062	7.373×10^{-4}
-1	-1 mm	0,769	1055	7.289×10^{-4}
-2	-2 mm	0,751	1053	7.132×10^{-4}
-3	-3 mm	0,660	1057	6.244×10^{-4}

Table 5.4: Test 2 results for circular lens in F.L.=Z-2

N Position Z-2 (F.L. 70 mm)				
N Position	X Positions (mm)	P (W)	S.R. (W/m^2)	P/S.R.
3	3 mm	0,671	1087	6.173×10^{-4}
2	2 mm	0,743	1075	6.911×10^{-4}
1	1 mm	0,784	1083	7.234×10^{-4}
0	0 mm	0,808	1077	7.502×10^{-4}
-1	-1 mm	0,792	1093	7.246×10^{-4}
-2	-2 mm	0,740	1073	6.896×10^{-4}
-3	-3 mm	0,684	1078	6.345×10^{-4}

Table 5.5: Test 2 results for circular lens in F.L.=Z-3

N Position Z-3 (F.L. 71,1 mm)				
N Position	X Positions (mm)	P (W)	R.S. (W/m^2)	P/S.R.
3	3 mm	0,681	1097	6.2079×10^{-4}
2	2 mm	0,852	1082	7.874×10^{-4}
1	1 mm	0,828	1088	7.610×10^{-4}
0	0 mm	0,819	1081	7.576×10^{-4}
-1	-1 mm	0,831	1077	7.716×10^{-4}
-2	-2 mm	0,830	1085	7.650×10^{-4}
-3	-3 mm	0,740	1073	6.896×10^{-4}

Table 5.6: Test 2 results for circular lens in F.L.=Z-4

N Position Z-4 (F.L. 72,2 mm)				
N Position	X Positions (mm)	P (W)	S.R. (W/m^2)	P/S.R.
3	3 mm	0,633	1074	5.894×10^{-4}
2	2 mm	0,787	1063	7.403×10^{-4}
1	1 mm	0,846	1072	7.892×10^{-4}
0	0 mm	0,781	1084	7.205×10^{-4}
-1	-1 mm	0,834	1081	7.715×10^{-4}
-2	-2 mm	0,818	1072	7.631×10^{-4}
-3	-3 mm	0,757	1064	7.115×10^{-4}

In order to facilitate the analysis of the results, two graphics with all the data are presented. The first graphic compares the $P/S.R.$ value for each z position in function of the x misalignments, as it is shown in Figure 5.1. The other graphic, in Figure 5.2, represents the $P/S.R.$ for each x displacement in function of the z position.

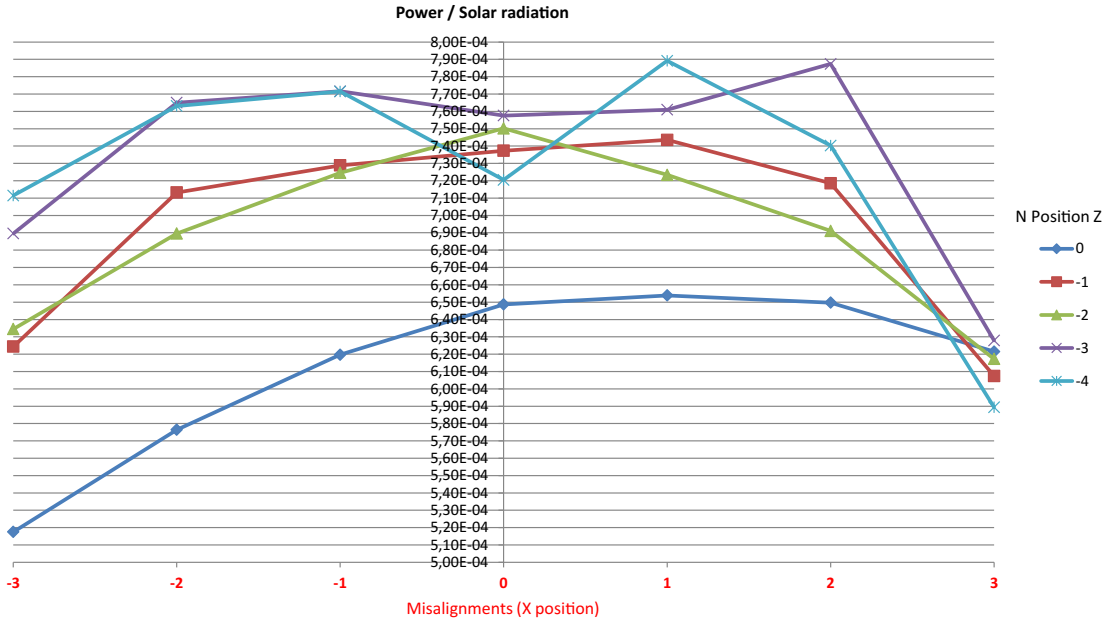

Figure 5.1: $P/S.R.$ value for each z position in function of the x misalignments.

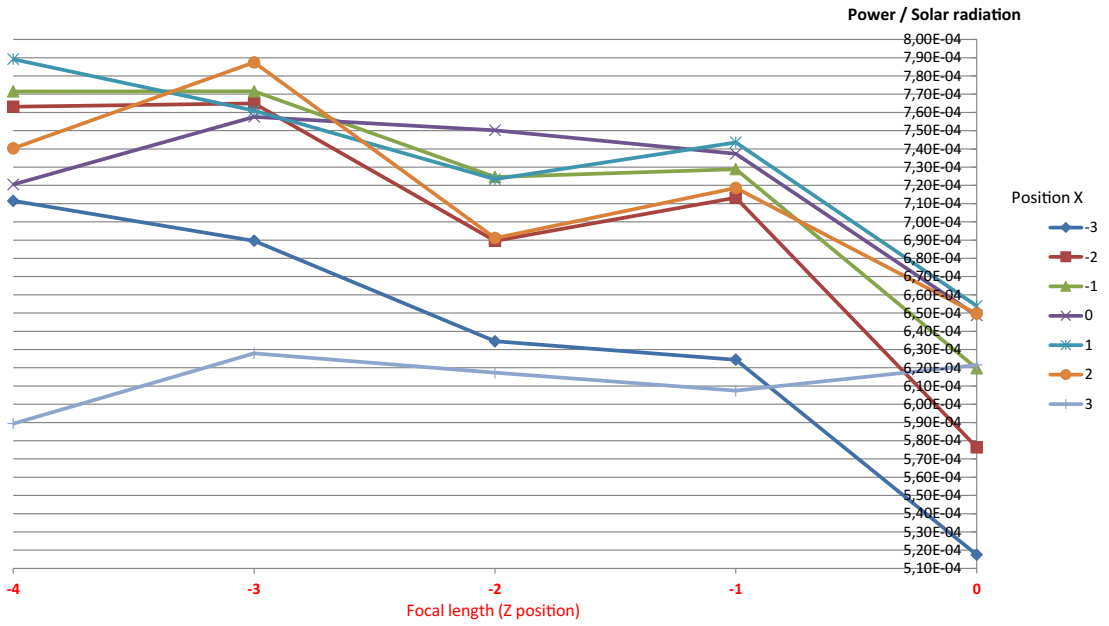

Figure 5.2: $P/S.R.$ (for each x displacement in function of the z position.

5.1.2.2 Square Fresnel lens

The test with square Fresnel lens presented some difficulties for the data collection process, specifically for simulating the x, y axes misalignments, since the system has a high sensitivity to flat misalignments and the precision of the solar alignment of the module affects the stability of the sensed values. Also, the visual alignment centering of the light spot in the area of the cell was not corresponding with the maximum power value. For all focal lengths tested, the higher power value was obtained positioning the light spot in a border of the solar cell, approximately 2,75 mm of x, y axes misalignment, near to the connecting paths as it is shown in Figure 5.3.

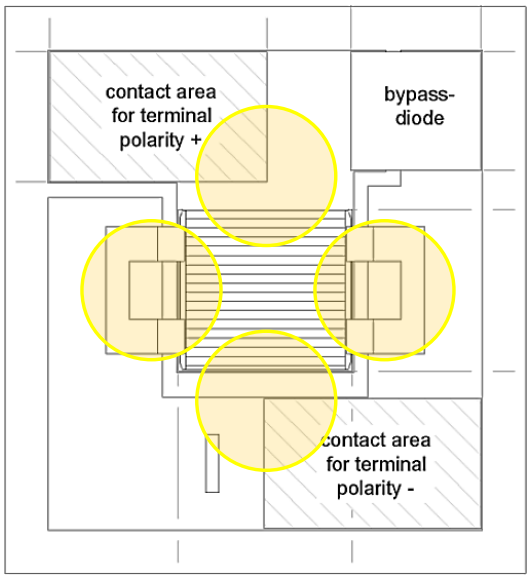

Figure 5.3: Observed light spot positions of maximum power generation with square Fresnel lens.

Despite the sensitivity of the system, a maximum power data in function of some focal lengths could be taken. The results are presented in Table 5.7 and plotted in Figure 5.4. The system sensitivity in flat misalignment (x, y) was approximately 0,3 mm.

Table 5.7: Test 2 results of maximum power for some focal Lengths for square lens

N Position Z Square Lens				
N position Z	Z position F.L. (mm)	Max P (W)	S.R. (W/m2)	P/S.R.
3	170,3	1,292	1089	0,00119
1	172,3	1,394	1089	0,00128
0	173,3	1,413	1088	0,00129
-1	174,3	1,422	1086	0,00131
-3	176,3	1,348	1086	0,00124

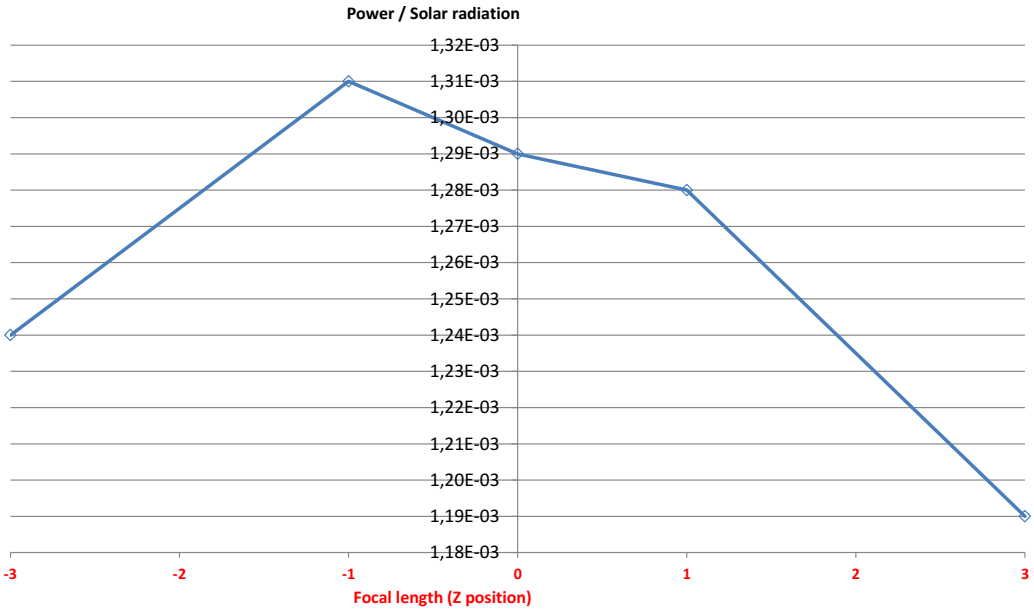

Figure 5.4: Test 2 plot results of P/Rad value for some focal lengths position for square lens.

5.1.2.3 Test 2 results analysis

- It is evident that the power increases with a higher focal length or distance of the cell regarding the lens (negative z with 0 in x, y axes). However, from a specific position the power decreases again. The reason of this behavior can be explained because of the chromatic aberrations generated by the lens. These aberrations create a concentration cone in which the different light spectra have different focal distances. After each spectrum exceeds its focal length, the cone of light is reversed as it is shown in figure 5.5 [16] [13]. This can increase the cell catchment of the other wavelengths through misalignments in the "z" axis, while the cell is closer to the

focal point of each wavelength (Infra-red with negative Z and Ultra-violet with positive Z). The light cone of the infra-red spectrum is similar to the visible spectrum but with higher focal length, so, lower z values represent greater focus of the infra-red spectrum on the cell. This spectrum is more useful for this, according to the cell data-sheet in Figure 5.6 [29]. Then, when the z displacement overcomes the range of infra-red focus the power generation is reduced again.

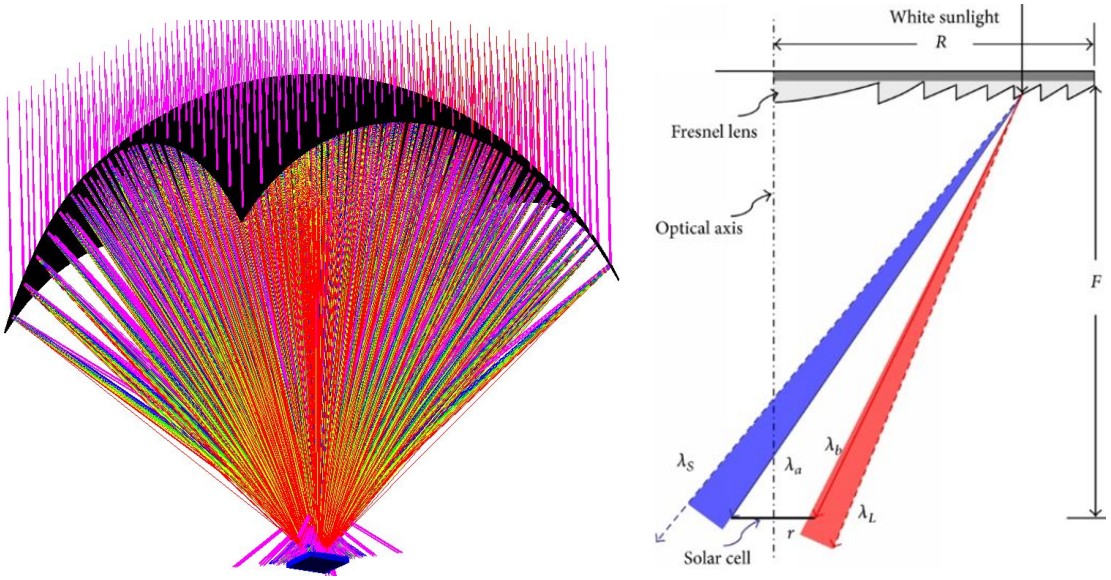

Figure 5.5: Chromatic aberration phenomenon presented in CPV system.[16] [13]

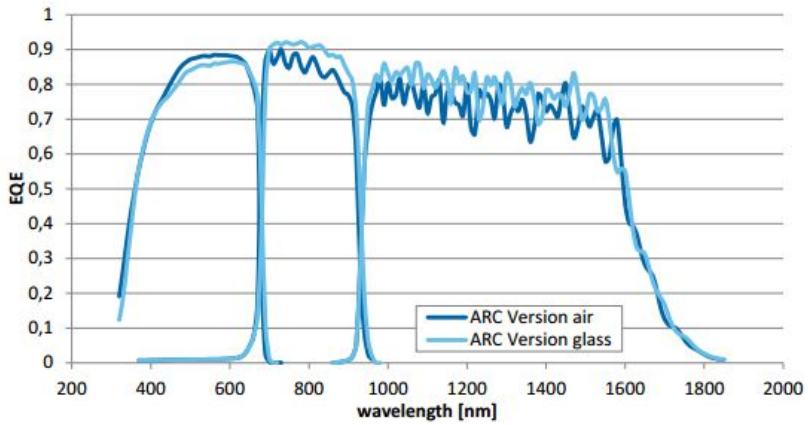

Figure 5.6: Spectral response (external quantum efficiency) of the cell used with different antireflective coating (ARC). [29]

- For the case of the circular lens, due to the large diameter and low focal length, the 1 mm step between each z position represents a higher distance proportion regarding the focal length and

a higher difference in the light spot, allowing to reach the light cone reverse, as it is shown in Figure 5.7, unlike the square lens, which present a higher focal length and lower diameter. As it is represented in Figure 5.8, the analysed focal lengths with 1 mm step do not allow to reach the light cone reverse and there could be more power generation in other z positions.

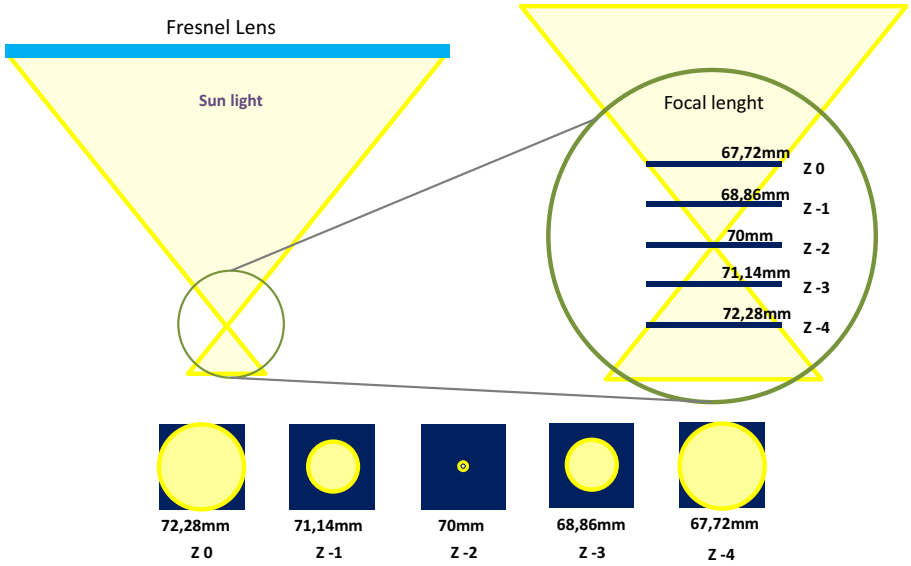

Figure 5.7: Light cone for circular lens and its implication in the light spot projected on the cell.

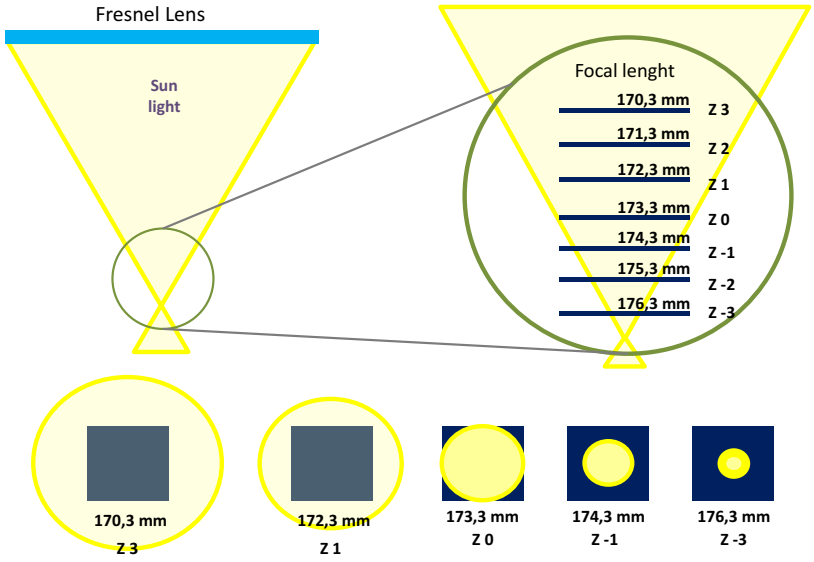

Figure 5.8: Light cone for the square lens and its implication in the light spot projected on the cell.

- With the circular lens the theoretical efficiency of the used elements, according to the manufacturer data, should be approximately 29%, cell efficiency of 40,5%, lens efficiency of 80% and electrical components efficiency of 90%. This efficiency should represent a generated power of 6,20 W with a Concentration factor (S) of 1012,4 and a DNI of 695 W/m^2, according to Equation 3.1. However, the maximum power registered is 0,852 W. To verify the lens efficiency, the F Number (focal length/diameter) was calculated. With a diameter of 175 mm and a focal length of 70 mm, the F Number of these lenses is 0,4. Nevertheless, the F Number curve does not present an efficiency range for this value. Now, assuming correct the cell efficiency of 40,5% due to temperature effects and the system efficiency of 90%, it is possible to calculate the lens efficiency with Equation 5.1, derived from Equation 3.1.Then, the lens efficiency will be 10,98% implying that more than 89% of the solar radiation does not come to the cell. This can be caused by low transmittance or manufacture defects, and mainly by chromatic aberrations, since the lens can present a good transmittance level for most of the wavelengths, but, due to chromatic aberrations the cell can not receive the whole light spectrum in a same position regarding the focal length.

$$\eta_{Opt} = \frac{Real\ Power}{A_C * S * DNR * \eta_{cell} * \eta_{Sys}} \tag{5.1}$$

- The power production with the square lens is 1,42 W, 66,6% more than circular lens. Considering F Number curve, the square lens efficiency should be approximately 92%. However, with Equation 5.1 the square lens efficiency is 42,4%. Due to the limitations with z axis positions for test 2, the maximum power production could be in a not analysed position, resulting in a higher efficiency of the lens.
- For the generation of the curves Power vs. Cell position, it is recommended to have a continuous measure of the variables in order to obtain the power production with a continuous displacement of the cell and generate a smooth curve with a deeper sensibility and more values for defining the internal tolerances because the usual tolerances of the tools and machines used for the manufacture of the systems are presenting in ranges of micron or tenths.

5.1.3 Test 3 results

For this test the CPV was in a static position for 10 minutes, the test was performed 3 times and data of Current, voltage, Solar radiation and temperature were taken. The results for circular lens are presented in Table 5.8 and plotted in Figure 5.9.

Table 5.8: Test temperature table results for circular lens

Temperature Test Circular lens				
Time (min)	P (W)	S.R. (W/m^2)	P/S.R.	T (°C)
0,5	0,700	1000	7.01×10^{-4}	46,3
1	0,698	997	7.00×10^{-4}	47,5
1,5	0,698	996	7.01×10^{-4}	48,3
2	0,695	1015	6.85×10^{-4}	46,9
2,5	0,602	1030	5.85×10^{-4}	48,2
3	0,695	1035	6.71×10^{-4}	49
5	0,694	1013	6.86×10^{-4}	56
7	0,692	1044	6.63×10^{-4}	54,3
10	0,688	1032	6.66×10^{-4}	58,2

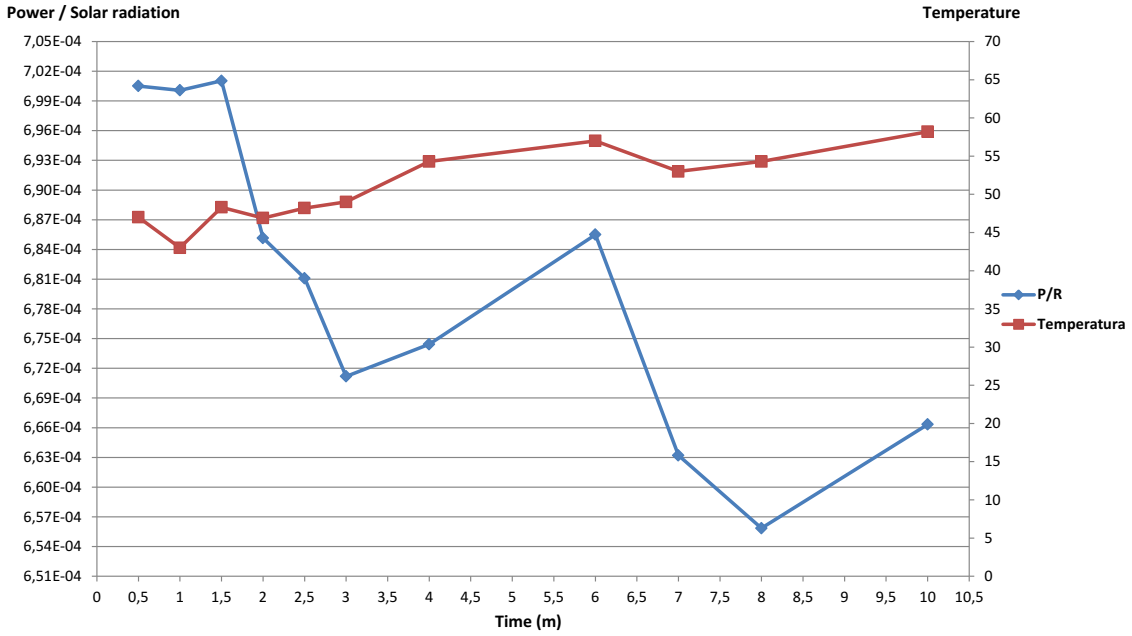

Figure 5.9: Test temperature plot results for circular lens.

For square lens, the measured power presented some problems due to the misalignment sensitivity of the system. However, data of maximum temperature level in function of the solar radiation are taken and the measurements are present in Table 5.9.

Table 5.9: Test temperature table results for square lens

Temperature Test Square lens		
Time (min)	S.R. (W/m^2)	T (°C)
0,5	1067	37
1	1076	40,6
1,5	1074	43
2	1064	44
2,5	1072	45,3
3	1080	49,2
5	1073	51,8
7	1071	52
10	1077	52

5.1.3.1 Test 3 results analysis

- In a specific time of 10 minutes the temperature achieves a maximum value of 58,2 °C for circular lens and 52 °C for square lens, the cell manufacturer gives a theoretical curve of efficiency in function of the concentration factor and different temperatures showed in Figure 5.10. The concentration factor for circular lens is 1012,4 and for square lens is 437 resulting in an efficiency of approximately of 39% for circular lens and 40,5% for square lens according the curve.

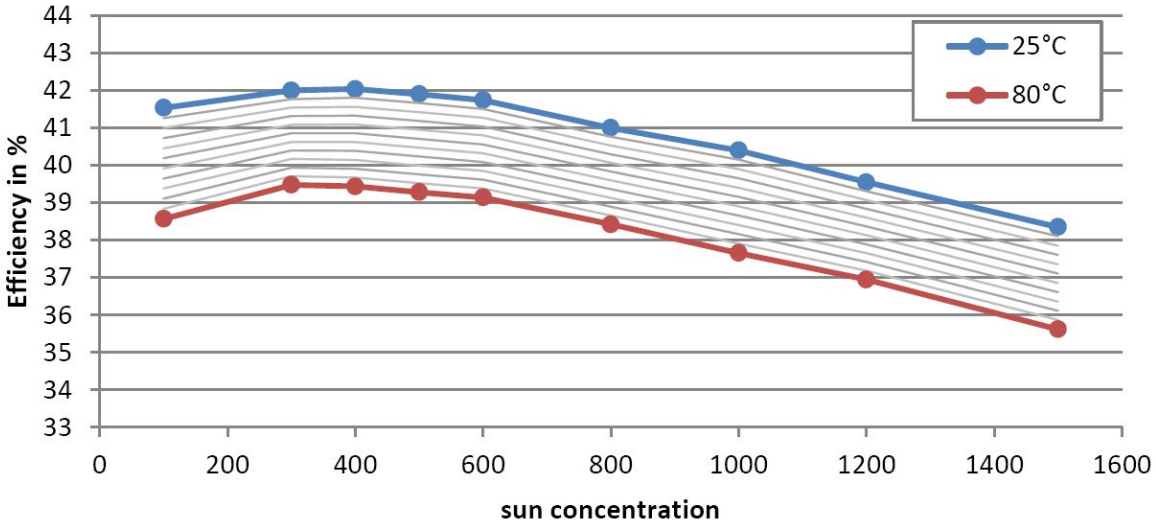

Figure 5.10: Data sheet of the cell behavior in function of different work temperatures.

- The system presents a common behavior where the temperature is inversely proportional to the the power generation. The power reduction can be explained with the loss efficiency of the cell by high temperature and lens deformations by thermal dilatation, resulting in a displacements of the focal points.

5.2 Theoretical implementation of the process results

5.2.1 Practical case results: Recalculation of CPV system power for WSC

According to Equation 3.12, the first step to recalculate the power of a defined CPV system is to obtain the characterizations curves of interaction with a real test of a cell-lens combination and to calculate the PI value. For this case, the data is obtained from Test 2 results of square Fresnel lens, which was performed with the same elements of the CPV system designed. The theoretical power of the CPV was calculated in 4,6 W and the real measured power was 1,42W, resulting in a PI of 0,309.

With the PI value, next step is to determine the forces that are supported by the system in order to determine the deflection levels. In this case, the force produced by the weight of the system (78,5 N) overcomes the wind force (65,6 N). Then, the analysis has to be performed with this force.

The inertia of each module was calculated dividing its cross section in basic geometries (rectangles, squares, circles, etc.) in order to calculate each inertia value and sum them for the resultant inertia. In total, three shapes are obtained, the base of the modules like an horizontal rectangle, the borders like vertical rectangles and the inertia of the lens array taking the T shape of the aluminium profile which sticks the lenses. With all the data, the deflections and TR were calculated. The results of the analysis are presented in Table 5.10.

Table 5.10: Analysis of the CPV system designed for WSC

Module 1		Module 2	
Length	1035 mm	Length	920 mm
Weight	4,23 Kg	Weight	3,77 Kg
Distributed force (W)	4.1×10^{-2} N/m	Distributed force (W)	4.2×10^{-2} N/m
Geometrical inertia	65535 mm^4	Geometrical inertia	65535 mm^4
Rigidity modulus (E)	145,4 GPa	Rigidity modulus (E)	145,4 GPa
Z Deflection	0,604 mm	Z Deflection	0,378 mm
Z tolerance process	0,5 mm	Z tolerance process	0,5 mm
Z total tolerance	1,103 mm	Z total tolerance	0,88 mm
X,Y deflection	1.7×10^{-4} mm	X,Y deflection	7.75×10^{-5} mm
X, Y tolerance process	0,5 mm	X, Y tolerance process	0,5 mm
X,Y total tolerance	0,5 mm	X,Y total tolerance	0,5 mm
System tolerance X, Y	0,3 mm	System tolerance X, Y	0,3 mm
System tolerance Z	1 mm	System tolerance Z	1 mm
Tolerance Ratio X, Y	0,6	Tolerance Ratio X, Y	0,6
Tolerance Ratio Z	0,9	Tolerance Ratio Z	1

The solar radiation value included in the TP calculation corresponds to the DNI calculated with Equation 3.13, which is 696 W/m^2.

Since the CPV system is divided in two modules supported from the center, the TP was calculated for each one. According to Equation 3.12, the TP for the first module, with length of 1035 mm, is 45,78 W, and for the second module, with length of 920 mm, is 30,94 W, resulting in a total theoretical production of 76,72 W of the whole system.

The TP value suggests an average power per CPV of 1,278 Wd which compared with the maximum power tested in the alignment controlled single CPV represents a power loss of 10% because of tolerances and alignments errors and uncontrolled variables presented during the implementation of the CPVs modules.

5.2.2 Theoretical case results

The theoretical design test allowed to recollect information about the ease of understanding, usability and application of the methodical process. The design process could not be finished due to doubts

raised by test users related with some data calculations and step sequence.The main statements done by the test users are summarized and listed in the following:

- The methodology text given is very extensive and difficult to understand.
- Include the calculation of the instantaneous power for both the average solar radiation and energy requirements.
- Indicate clearly how the environmental conditions can affect the system performance.
- The step sequence given presents indeterminate variables for the equations use, its generates many reprocess in the calculations.

The results of this test suggest to redefine the whole steps sequence of the methodical process and specify some determinate values and concepts for calculations, in order to do the corrections. The theoretical case was done redefining the methodical process in such a way that the sequence and calculations are more fluid. Then, all the changes will be integrated to redefine the process in an infographic format.

5.2.2.1 Development of the theoretical case

1. **Conceptual design:**
   - **PDS:**
     - **Power requirements:** 3,5 KWh per day, with 6 sun hours represents 584 W of instant power.
     - **Space restriction:** Deployment area of 100 m^2 - 60 m^2 = 40 m^2. Storage volume of 1250 mm x 1600 mm x 350 mm representing an area of 2000 mm^2.
     - **Environmental conditions** The average instant solar radiation in the context will be 4500 Wh/m^2 / 6 sun hours = 750 W/m^2.
   - **Component selection**
     - For this case, the components are given.
     - The concentrator factor will be 1071.
     - The F number value of the lens used is 0,39. This value is not included in the F number efficiency curve.
     - Assuming a lens efficiency of 80% and an electrical system efficiency of 90%, the initial power calculation is: 0,00003025 m^2 * 1071 * 750 W/m^2 * 42%*80%*90% = 7,34 W
   - **Module division:**
     - **CPV quantity for power:** 584 W / 7,34 W = 80 CPVs.

- **CPV quantity for areas:** 40 m^2 / 0,0342 m^2 = 1170 CPVs.
- **Module division for area:**
  - To determine the CPV quantity for power: 80 CPVs*0,0342 m^2 / 2 m^2 = 1,37 = 2 modules.
  - To determine the CPV quantity for areas: 40 m^2 / 2 m^2 = 20 modules

2. **Characterization:**

- The characterization of interaction was given indicating a maximum power production of 3,57 W. With this data, the PI is 0,486.
- with a z axis misalignment of 1 mm, the power is reduced in 3,5%.
- with a x misalignment of 0,5 mm, the power is reduced in 18%.
- **Recalculating the Module division:**
  - Recalculating the CPV quantity with the real maximum power, the new CPV quantity will be: 584W / (7,34 W * 0,486) = 164 CPVs
  - The new deployment area for 164 CPVs will be 5,31 m^2.
  - The minimum number of modules with new areas will be 2,65 = 3.

3. **Detail design:**

- **Material selection:** Steel is selected due to its cost-mechanical properties ratio, with a Rigidity modulus (E) of 220 GPa and density of 7850 Kg/m^3.
- **Module geometrical design:**
  - **Deployment height:** According to interaction characterization data, the useful focal length is 67,5 mm, then, the deployment height for the modules is 67,5 mm height + 3 mm of lens thickness + 3 mm of theoretical maximum thickness of the module base will be 73,5 mm.
  - **Storage area:** The available storage area is 2 m^2, however, the lens area is a fixed value, for this reason, it is important to determine the lengths sides of the modules through CPV number combinations. Knowing that the minimal length side for any module has to be 1,25 m and the maximal one 1,6 m, the only available combination to reach the maximum CPVs quantity in a module is 48 CPVs (8 x 6 CPVs), which, with a lens side of 0,182 m, the total lengths sides are 1,44 m and 1,08 m. Now, to reach the 164 CPVs needed for the power requirements in the minor module quantity, the modules quantity have to be 4 modules: 3 modules of 48 CPVs and 1 module of 20 CPVs (5 x 4 CPVs) with length sides of 0,9 m and 0,72 m, respectively.

- **Storage height:** The storage height of 4 modules by stacking is (67,5 mm + 3 mm + 3 mm) * 4 = 294 mm, available for the maximum storage limit of 350 mm.

- **Forces calculation:**

  * **Weight force:** To determine the weight force is necessary to calculate the weight of each module in order to identify the maximum weight levels, deflection levels and guarantee the property behavior of the other modules.

    In the case of the chassis weight, it is possible to approximate the volume of the basic module design, considering a thickness of 3 mm.

    For 1, 2 and 3 modules, the volume of each one is the sum of the volume of the module base which is 1,55 m^2 * 0,003 m = 0,0046 m^3, and the volume of the edges which are (1,44 m * 0,0675 m * 0,003 m)*6 = 0,0017 m^3 and (1,08 m * 0,0675 m * 0,003 m) * 6 = 0,0013 m^3, resulting in a total volume of 0.0076 m^3 for each module. Then, the weight of each one will be 59,6 Kg + 2,3 Kg by cell and lens weight: 61,9 Kg.

    For module number 4, the volume of the module base is 0,648 m^2 * 0,003 m = 0,00194 m^3, and the volume of the borders will be (0,9 m * 0,0675 m * 0,003 m)*2 = 0,00036 m^3+ (0,72 m * 0,0675 m * 0,003 m)*2 = 0,00029 m^3, for a total volume of 0,0026 m^3. Then, the weight of the fourth module is 20,3 Kg + 0,98 Kg considering cells and lenses weight: 21,28 Kg.

    The theoretical weight of the whole system will be approximately 207 Kg, available for the vehicle load capacity of 375 Kg.

    Finally, for this case, the largest module (1, 2 and 3) presents higher deflections values. Then, the used value of the mass is 61,9 Kg representing a force of 584,7 N.

  * **Wind force:** The calculated wind force for the context of use with major average wind speed is 115,5 N, with an air density of 1,16 Kg/m^3, DA of 1,55 m^2 and wind speed of 8 m/s.

  * According to the results, the inertia analysis has to be done with the higher force value: 584,7 N.

- **Inertia calculation**

  The inertia of the basic module design is given mainly by 2 of its borders which have dimensions of 0,0675 m of height and 0,003 m of base, resulting an inertia per module of 1/12 * 0,003 m * (0,0675 m) ^{3}= 7.6×10^{-8} m^4 *2 = 1.53×10^{-7} m^4 or 153773,43 mm^4.

The maximum theoretical deflection of a module with the calculated inertia is 3.14×10^{-6} mm. Then, the deflection in z axis is 0 and, therefore, the displacements in x, y axes will be 0.

For the high rigidity level of the module, it is possible to reduce the selected thickness of 3 mm, reducing the weight of the system.

- **Manufacture process selection:**

  Searching a CPV system tolerance ensuring a maximum power loss of 2%, the maximum z axis misalignment should be 0,5 mm and the maximum x, y axes misalignment should be 0,05 mm. Now, the manufactured process selected for module manufacture in steel is milling, presenting an error of 0,03 mm and an error of 0,1 mm for hole cutting.

- **Assembly strategy selected:**

  Knowing the milling tolerances, the assembly centered in the interface element is selected, in order to speed up the process.

- **Tolerance ratio:**

  The TRz will be 0,5 mm / 0,03 mm = 1.

  The $TRxy$ will be 0,05 mm / 0,1 mm = 0,5.

4. **Theoretical energy production calculation.**

   The DNI for the theoretical energy calculation is approximately 750 W/m^2 * $0{,}7^{1{,}09^{0{,}678}}$ = 514 W/m^2.

   The TP is 0,00003025 m^2 * 1071 * 514 W/m^2 * 0,486 * 90% * 164 * 0,5 * 1 = 597,3 W, satisfying the energy requirements.

5.2.2.2 Methodical Process Sequence Redefinition

Considering the methodical process application, some changes in the step sequence are suggested. The following list summarizes all the steps of the methodical process together with the used equations according to the suggested definitions in the theoretical case application.

1. **Conceptual design:**

   - **PDS:**
     - **Power requirements:** To calculate the instant power from an energy requirement, the energy value given is divided by the sun hours of the day.
     - **Space restriction:** Dimensions, areas and volumes for storage and deployment.

- **Environmental conditions** In additions to the temperatures, humidity levels, precipitation levels, and wind forces, the average instant solar radiation in the context can be calculated dividing the historic energy value of the context by the sun hours. Then, the DNI value can be obtained with Equation 5.2 and 5.3.

$$DNI = Total\ Solar\ Radiation * 0,7^{AM^{0,678}} \tag{5.2}$$

$$AM = \frac{1}{cos(\theta)} \tag{5.3}$$

- **Component selection**
  - The concentrator factor should be defined to know the areas of the components.
  - Define the F number of the used lens with Equation 5.4, to obtain an efficiency level from the F number curve.

$$F\ number = \frac{Focal\ length}{lens\ diameter\ or\ diagonal} \tag{5.4}$$

- **Theoretical power calculation**

  Calculate a theoretical power production of the system with Equation 5.5.

$$E = (A_c * C.F. * DNI * \eta_c * \eta_{op} * \eta_s * N_{CPV}*) \tag{5.5}$$

2. **Characterization:**

- Perform the interaction characterization to determine the system sensitivity and the maximum power level related with a specific position.
- Determine the power reduction for the minimum misalignment step in z axis.
- Determine the power reduction for the minimum misalignment step in x, y axis.
- Calculate the PI value with real measured power and the first theoretical power value with Equation 5.6.

$$PI = \frac{Real\ power}{Theoretical\ power} \tag{5.6}$$

3. **Module geometrical design:**

- **Material selection:** Select the materials and determine a Rigidity modulus and a density, for an initial calculation of the weight.
- **Module geometrical design**

- **Module division**
  - Calculate the CPV quantity with Equation 5.7, using the real power tested in the interaction characterization and the requirements power.

$$N_{CPV} = \frac{W_{needed}}{W_{mpp}} \tag{5.7}$$

  - Determine the deployment area with Equation 5.8, considering the calculated quantity of a CPV and the fixed lens area.

$$N_{CPV} = \frac{Deployment\ area}{Lens\ area} \tag{5.8}$$

  - Without power restrictions, the CPV quantity can be limitated by a deployment area.

- **Maximum module dimension**

  Determine the minimum quantity of modules with Equation 5.9. Since the lens dimensions are fixed values, the largest module with more CPVs quantity can not overcome the storage dimensions as it is indicated in Equation 5.10 and Equation 5.11.

$$N_{Modulos} = \frac{Deployment\ area}{Storage\ area} \tag{5.9}$$

$$Lens\ side\ 1 * X\ CPV\ quantity \leq Storage\ dimension\ 1 \tag{5.10}$$

$$Lens\ side\ 2 * Y\ CPV\ quantity \leq Storage\ dimension\ 2 \tag{5.11}$$

- **Module dimensions:**
  - **Deployment height:** Select the useful focal length according to interaction characterization data and sum the lens thickness and a theoretical maximum thickness of the module walls.
  - **Storage area:** Identify the area of the largest CPV module calculated in Module division part.
  - **Storage height:** According to the storage limitation, the storage height can be defined by stacking such as in Equation 5.12 or develop modules with variable height.

$$Storage\ Height\ (S.H.) = Deployment\ Height * modules\ quantity \tag{5.12}$$

- **Forces calculation:**
  - **Weight force:** Calculate the weight of each module, considering a basic geometry of tray shape, in order to identify the maximum weight levels, deflection levels and guarantee the property behavior of the other modules. In the case of the chassis weight, it is possible to approximate the volume of the basic module design, considering the areas of all its faces (base and walls) and the thickness value selected before. Then, the total volume is multiplied with the selected material density, and the weight of cells and lenses presented in the module are summed.
  - **Wind force:** Calculate the maximum wind forces with the largest module dimension with Equation 5.13.

$$WindF = \frac{1}{2} * \rho * D.A. * Cd * W.Speed^2 \tag{5.13}$$

- **Deflection calculation:**

  The detail design has to define the values for the maximum deflection levels with equation 5.15:

  According to the force calculation results, the inertia analysis has to be done with the higher force value between weight force and wind force.

  The inertia of a basic module design is given mainly by 2 of its borders which have rectangular shape and specific dimensions of base and width for the inertia calculation with Equation 5.14. Then, it is possible to determine the module deflection levels with Equation 5.15, and the lateral displacements through Equation 5.16 with the material rigidity and the inertia calculated and to add geometrical elements if needed.

$$I\ rectangular\ shape = 1/12 * base * height^3 \tag{5.14}$$

$$\delta max = \frac{-w * L^4}{8 * I * E} \leq z\ system\ tolerances \tag{5.15}$$

$$x, y\ displacements = (\frac{length}{sin(tan^{-1}(\frac{\delta max}{length})}) - length \tag{5.16}$$

- **Manufacture process selection:**

  Determine a manufacturing process according to the internal tolerances of the system and the tolerances of the process.

- **Assembly strategy selected:**

  Select the assembly strategy considering the alignment errors and the internal tolerances of the system.

4. **Theoretical Power production.**

   - **Tolerance ratio:**

$$TR = \frac{Internal\ tolerances}{Process\ tolerances + deflections\ tolerances} \leq 1 \tag{5.17}$$

     – Determine the TRz summing the deflection value, the z tolerances of the process and the z alignment tolerances.

     – Determine the $TRxy$ summing the displacements produced by the deflection, the x, y tolerances of the process and the x, y alignment tolerances.

   - **Theoretical power production calculation**

$$TP = (A_{cell} * N_{sun} * DNI * PI * \eta_{sys} * N_{CPV}) * (TR_{x,y}) * (TR_z) \tag{5.18}$$

Figure 5.11 presents an infographic in order to facilitate the use of the methodical process and summarize the whole process.

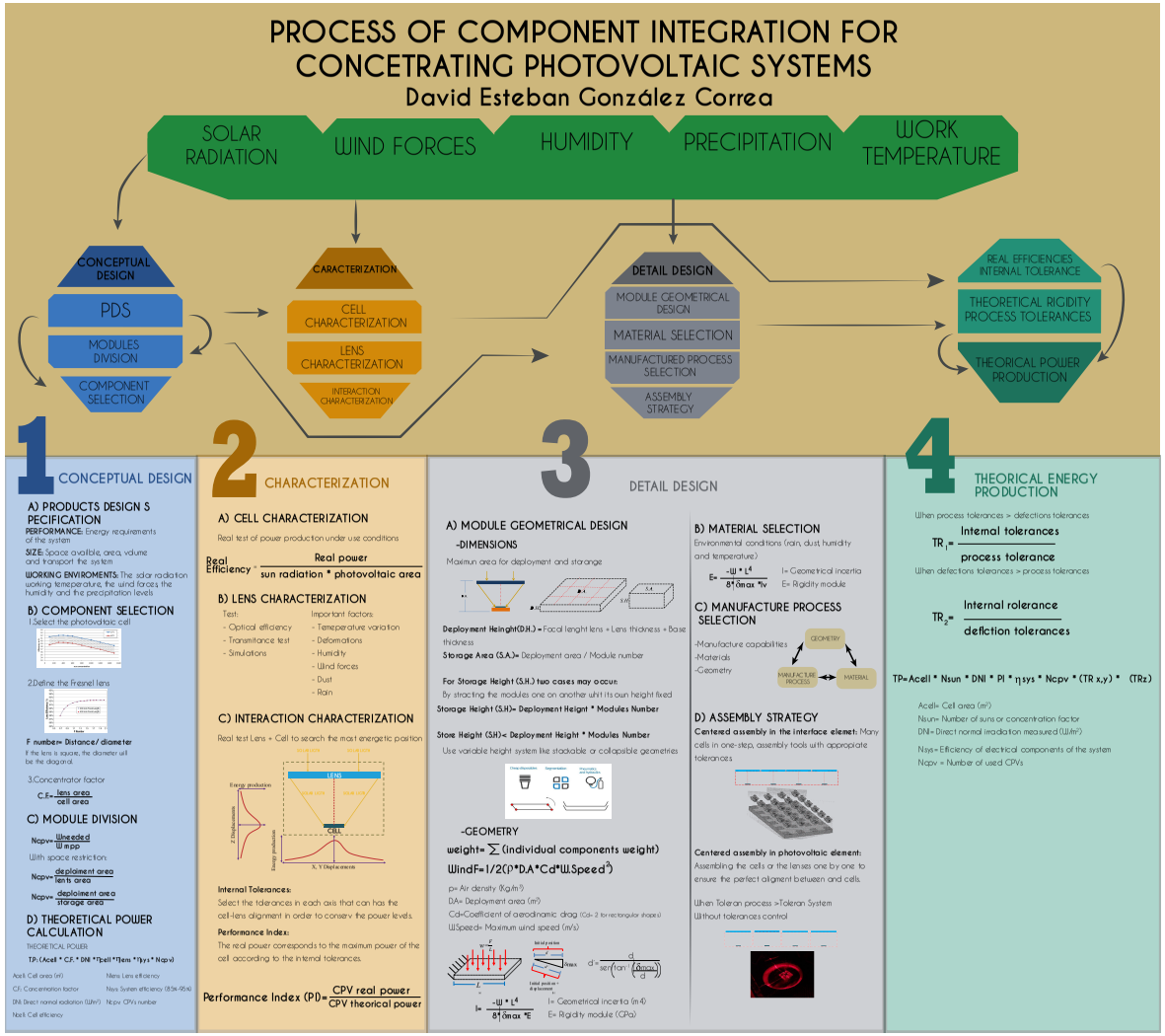

Figure 5.11: Infographic summarizing the methodical process proposed

Chapter 6

Conclusions

- The proposed process is specific for CPV systems with Fresnel lenses. However, its main steps can be easily adapted to systems using other optical elements, mainly, by adjusting the selection parameters of the optical component and defining ways to characterize components and correct assembly processes.

- The power calculation results can vary significantly because of the way in which the design process is developed. The proposed approach is presented only as a suggestion of steps to improve the prediction of the behavior of systems before running the construction design. However, in some cases, acquisition of some components to perform real tests such as internal tolerances of the lens-cell integration might not be viable, and for these cases, the appropriate use of secondary lenses can provide a lower sensitivity of the system against displacement. It is also recommended to carry out a deep search of simulation methods for different cases and required components.

- Main environmental variables that affect energy production of a CPV are presented as time changing variables that may or may not adversely affect the system at a specific time. The temperature is a variable that can be easily characterized and integrated as a constant environmental variable in the interaction of the components. However, the relative humidity and the level of precipitation suggest the implementation of levels of protection or impermeability according to the most extreme case, since, through these protections, the effect of these variables can be ignored.

- For both tests, in the performance index test 2, a higher focal length regarding the theoretical initial position improves the power production of the cell, for this reason it is import to perform the interaction characterization test.

- A major F number of lens (higher focal length and minimum lens diameter), allows greater displacements in Z axis due to the closed angle of the light triangle.
- The Performance Index (PI) represents the deviation of a first theoretical power approach and a real tested power value. Nevertheless, this ratio can be used to calculate the deviation of the final theoretical power, obtained through the methodical process with the real power of the CPV system design finished and built, in order to know the adjustment of the new theoretical value.
- For practical case test, the case with the solar vehicle CPV system, the recalculation of the system power including the PI value and the TR is really closed to the average power sensed under real use conditions with a PI between this calculation and the average power tested of 76,72 W / 75 W = 0,97.
- Another way to interpret the proposed theoretical power calculation could be such as the Equation 6.1, where η_{total} represent the whole efficiencies of the system affected by the environmental conditions. Then, to determine these efficiencies is not enough to know the real efficiencies of the CPV components because these are affected by the context conditions. In this way, it is necessary to determine appropriately the environmental variables and know how these affect the different efficiency levels of each component.

$$TP = (DNI * Lens\ area * \eta_{total}) * TR_z * TR_{xy} \tag{6.1}$$

- Further research is oriented to perform more practical cases using the proposed methodical process in order to validate its real advantages and to determine the error level between the theoretical power obtained through the process and the real performance of a CPV system designed using the process.

Bibliography

[1] Andrés Arias-Rosales, Jorge Barrera-Velásquez, Gilberto Osorio-Gómez, and Ricardo Mejía-Gutiérrez. Designing a concentrating photovoltaic (cpv) system in adjunct with a silicon photovoltaic panel for a solar competition car. In *SPIE Sensing Technology+ Applications*, pages 91150W–91150W. International Society for Optics and Photonics, 2014.

[2] W. Carr and S. Kemmis. *Becoming Critical: Education, Knowledge, and Action Research*. [EBSCO eBook Collection]. Falmer Press, 1986.

[3] Daniel Chemisana. Building integrated concentrating photovoltaics: a review. *Renewable and Sustainable Energy Reviews*, 15(1):603–611, 2011.

[4] CPV Consortium., sep 2013.

[5] DiYPRO., jan 2017.

[6] Kristine Drew, Nigel Morris, Michael Sinclair, Stefan Myrskog, and John Paul Morgan. Sensitivity analysis applied to a concentrator photovoltaic system. *Photovoltaic Specialist Conference (PVSC), 2014 IEEE 40th*, pages 2917–2920, 2014.

[7] Airlight Energy, feb 2008.

[8] David Fork, David Duff, Michael Weisberg, Thomas Zimmermann, and Stephen Horne. Solar concentrating photovoltaic device with resilient cell package assembly, May 5 2006. US Patent App. 11/382,004.

[9] Slava Hasin and Ron Helfan. Photovoltaic module assembly, May 29 2013. US Patent App. 13/904,251.

[10] Edmund Optics Inc., mar 2016.

[11] Morgan Solar Inc., may 2007.

[12] Sebastián E CAPARRÓS JIMÉNEZ, Antonio De Dios Pardo, Carlos Martín Maroto, Enrique JIMÉNEZ SÁEZ, and Adam Botts. Mounting procedure of a high-concentration photovoltaic solar module and module thus mounted, March 4 2013. US Patent App. 13/784,285.

[13] Lei Jing, Hua Liu, Yao Wang, Wenbin Xu, Hongxin Zhang, and Zhenwu Lu. Design and optimization of fresnel lens for high concentration photovoltaic system. *International Journal of Photoenergy*, page 7, 2014.

[14] Sarah Kurtz, Matthew Muller, Dirk Jordan, Kanchan Ghosal, Brent Fisher, Pierre Verlinden, Jun Hashimoto, and Daniel Riley. Key parameters in determining energy generated by cpv modules. *Progress in Photovoltaics: Research and Applications, vol. 23, no. 10,*, pages 1250–1259, 2015.

[15] Green Rhino Energy Ltd., apr 2013.

[16] mark o'neill., jan 2012.

[17] Etienne Menard, Christopher Bower, Scott Burroughs, Joe Carr, Bob Conner, Sergiy Dets, Bruce Furman, Matthew Meitl, and Michael Sullivan. Concentrator-type photovoltaic (cpv) modules, receiver and sub-receivers and methods of forming same, February 9 2010. US Patent App. 12/702,841.

[18] Wayne Miller, Victor Ocegueda, Jeremy Dittmer, Roger Sinsheimer, and Mike Prucha. Alignment of photovoltaic cells with respect to each other during manufacturing and then maintaining this alignment in the field, September 8 2011. US Patent App. 13/227,649.

[19] Rubén Mohedano, Aleksandra Cvetkovic, Pablo Benitez Gimenez, Juan Carlos Miñano Dominguez, Maikel Hernández Sanz, Pablo Zamora Herranz, and J Vilaplana. Wide-angle, high-concentration photovoltaics to compete with flat plate systems. *SPIE Newsroom*, pages 1–3, 2013.

[20] H Mughal. An innovative design of a low cost 120x concentrating system based on proven one sun technologies. In *Photovoltaic Specialists Conference (PVSC), 2009 34th IEEE*, pages 000781–000785. IEEE, 2009.

[21] Mattehew Muller. Experience with cpv module failures at nrel,. In *2012 Reliability Workshop, Golden CO*. NREL, 2012.

[22] Stephen Olah. Solar energy module and fresnel lens for use in same, June 4 2002. US Patent 6,399,874.

[23] Stuart Pugh. *Total Design: Integrated Methods for Successful Product Engineering*. Pearson United Kingdom, 1990.

[24] pveducation., jan 2016.

[25] Lanxu Ren, Xiudong Wei, Zhenwu Lu, Weixing Yu, Wenbin Xu, and Zhenfeng Shen. A review of available methods for the alignment of mirror facets of solar concentrator in solar thermal power system. *Renewable and Sustainable Energy Reviews, vol. 32*, pages 76–83, 2014.

[26] Steven Seel, Etienne Menard, David Kneeburg, Baron Kendrick, Bruce Furman, Wolfgang Wagner, Ray Jasinski, and Scott Burroughs. High concentration photovoltaic modules and methods of fabricating the same, December 5 2012. US Patent App. 13/705,980.

[27] Inc. Semprius, aug 2006.

[28] Soitec, feb 1997.

[29] Azur Space, apr 2014.

[30] WT Xie, YJ Dai, RZ Wang, and K Sumathy. Concentrated solar energy applications using fresnel lenses: A review. *Renewable and Sustainable Energy Reviews*, 15(6):2588–2606, 2011.